26

Quantum Calculation in Prediction the Properties of Single-Walled Carbon Nanotubes

Majid Monajjemi[1] and Vannajan Sanghiran Lee[2,3]
[1]*Department of Chemistry, Science and Research Branch, Islamic Azad University, Tehran,*
[2]*Department of Chemistry, Faculty of Science, University of Malaya, 50603, Kuala Lumpur,*
[3]*Computational Simulation and Modeling Laboratory (CSML),*
Thailand Center of Excellence in Physics, Commission on the Higher Education,
Ministry of Education, Bangkok,
[1]*Iran*
[2]*Malaysia*
[3]*Thailand*

1. Introduction

Since the first discovery of single-walled carbon Nanotubes (SWCNTs) by Iijima and Bethune in 1993 (Bethune et al., 1993), many applications as molecular components for nanotechnology including conductivity and high-strength composites; energy storage and energy conversion devices; sensors; field emission displays and radiation sources; hydrogen storage media; and nanometer-sized semiconductor devices, probes, and interconnects are known (Ajayan et al., 1994; Saito et al., 1997; deHeer et al., 1995; Collins et al., 1997; Nardelli et al., 1998; Huang et al., 2006). SWCNTs have been considered as the leading candidate for Nan device applications because of their one-dimensional electronic bond structure, molecular size, biocompatibility, controllable property of conducting electrical current and reversible response to biological reagents. Hence SWCNTs make possible bonding to polymers and biological systems such as DNA and carbohydrates. Most SWCNTs have a diameter of close to 1 nanometer, with a tube length that can be many millions of times longer. The average diameter of a SWNT is 1.2 nm (Spires & Brown, 1996). However, Nanotubes can vary in size, and they aren't always perfectly cylindrical. As in Fig. 1, the average bond length and carbon separation values for the hexagonal lattice were shown. The carbon bond length of 1.42 Å was measured by Spires and Brown in 1996 (Spires & Brown, 1996) and later confirmed by Wilder et al. in 1998 (Wilder et al., 1998).

The structure of a SWNT can be formed by the rolling of a single layer of sp^2 carbon, called a graphene layer, into a seamless hollow cylindrical tube with Nan scale dimensions of 1-1.5 nm. The length is usually in the order of microns to centimeters. Besides their unique physical properties (elasticity, tensile strength, stiffness, and deformation), Nano tubes exhibit varying electrical properties (depending on the direction that the graphite structure spirals around the tube (quantified by the "Chiral vector"), and other factors, such as doping), and can be superconductor, conductor (metallic), semiconductor or, insulator. The band structure can even be further manipulated, by introducing defects into a tube. Single-

walled nanotubes exhibit electric properties that are not shared by the multi-walled carbon nanotube (MWNT) variants. In particular, their band gap can vary from zero to about 2 eV and their electrical conductivity can show metallic or semiconducting behavior, whereas MWNTs are zero-gap metals. The C-C tight bonding overlap energy is in the order of 2.5 eV. Wilder *et al.* estimated it to be between 2.6 eV - 2.8 eV (Wilder et al., 1998) while at the same time, Odom *et al.* estimated it to be 2.45 eV (Odom et al., 1998). Multi-walled carbon nanotubes have a layer of carbon shells with differing physics that can all potentially interact. It is shown that only the outer shell of MWCNTs contributes to electrical transport, and so only small diameter MWCNTs could be used to make transistor devices. SWCNTs are the most likely candidate for miniaturizing electronics beyond the micro electromechanical scale currently used in electronics. As this field continues to expand and grow, materials technology will produce products, components and systems that are smaller, smarter, multi-functional, environmentally compatible, more survivable, and customizable. These products will not only contribute to the growing revolutions of information and biology, but will also significantly impact manufacturing, logistics, and our culture as a whole. The development of scanning probe techniques has allowed not only the microscopy of surfaces with atomic resolution, but also the manipulation of atoms and molecules on surfaces, and many analytical techniques have been developed to allow detailed characterization of materials and structures on the atomic level with unprecedented accuracy. The utilization of materials with nanometer-sized structures will lead to innovative products which are smaller, smarter, and more multi-functional. Therefore, understanding of fundamental properties of structures at the nano scale with the aid of computational models is important to design the specific material properties.

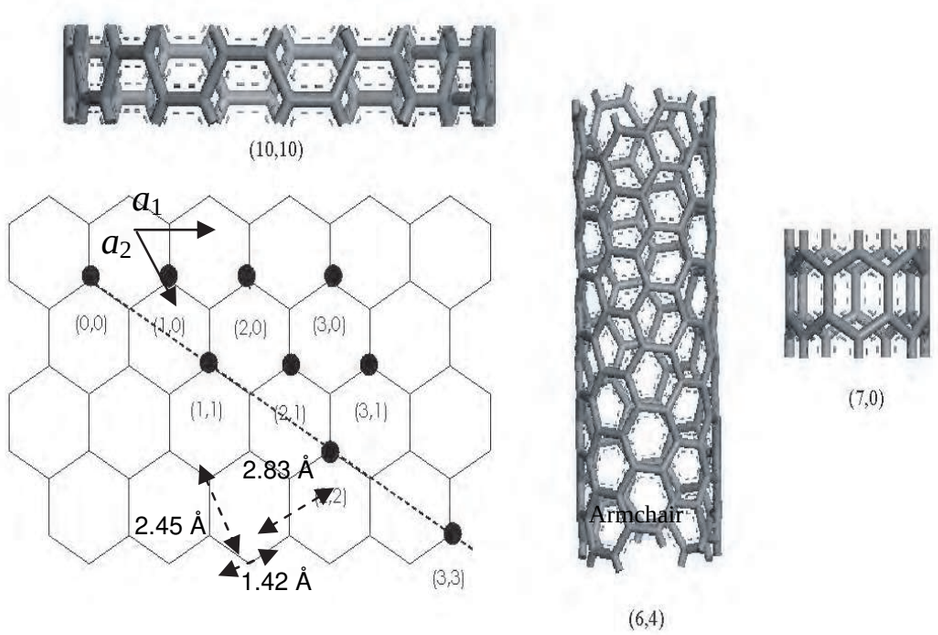

Fig. 1. The geometrical structure of SWCNT

Recently, theoretical and experimental work have predicted that the infinity length SWCNTs are Pi-bonded aromatic molecules that the electrical properties depending upon the tubular diameter and helical angle (Zhou et al., 2004; Baron et al., 2005). SWCNTs can be chiral or nonchiral, again depending on the way of the rolling up vector. As a graphene sheet was rolled in many ways in horizontal, vertical, and diagonal direction represent as arrow vectors, $\vec{a}$, as in Fig. 1, the different types of carbon nanotubes were produced. The three main types are armchair, zig-zag, and chiral nanotube. The geometrical and electronic structure of SWCNT can be described by a chiral vector, the angle between the axis of its hexagonal pattern and the axis of the tube which is presented by a pair of indices (n_1,n_2) called the chiral vector. The integers n_1 and n_2 denote the number of unit vectors along two directions in the honeycomb crystal lattice of graphene. When the indices are (n_1,*0*) called zig-zag, (n_1, n_1) called armchair, and (n_1, n_2) where $n_1 \neq 0$ *and* $n_2 \neq 0$ known as chiral SWCNT. For (2 n_1 + n_2)/3 = integer, SWCNTs are metallic and others are semiconductors (Saito et al., 1992a, 1992b). For large diameter SWCNTs defined by $d = \frac{\sqrt{3(n_1^2 + n_2^2 + n_1 n_2)}}{\pi} a_{c-c}$, where $a_{c\text{-}c}$ is the distance between neighboring carbon atoms in the flat sheet, armchair SWCNTs are always metallic which is good for nanotechnology application. A zigzag carbon nanotube (n_1, 0), is a semiconductor when $n_1/3 \neq$ integer. Such semiconductor zigzag carbon nanotubes have the ability to become base of many nanoelectronic devices and transistors.

Although, scientific efforts focused on the electrostatics properties and commercial applications of these materials (Ouyango et al., 2002; Kane & Mele, 1997; Hartschuh et al. 2005), there have been no experimental structural data sufficiently accurate for the identification of the chirality indices of SWCNTs, especially for the kind of smaller diameter nanotubes. In all experimental methods for the identification commonly utilized so far is Raman spectroscopy and phonon dispersion. Phonon dispersion relations in one dimension of this system have been studied by using zonefolding along one direction of Brillouin zone considering the tube symmetry (Eklund et al., 1995). The tight binding electronic band structure and the reverse of the diameter (1/*d*) dependence of the frequency of the radial breathing mode (RBM) were employed (Jorio et al., 2001; Bachilo et al, 2002; Pfeiffer et al. 2003; Kurti et al., 2004; Maultizsch et al., 2005). The size and chirality of the carbon nanotubes were typical determined from the SWCNT Raman energy spectra of a peak around 150–300 cm^{-1}, due to the radial breathing mode (Maultizsch et al., 2005; Jorio et al., 2005). Further Raman studies of SWCNT modified by various reactions e.g. oxidation reactions, ozonolysis, fluorination, residues modification (Srano et al., 2003; Umek et al., 2003; Peng et al., 2003; Bahr et al., 2001; Holzinger et al., 2003; Mickelson et al., 1998; Cai et al., 2002; Banerjee & Wong, 2002; Herrera & Resasco, 2003; Martinez et al., 2003) have revealed that covalent functionalization mainly affects the intensity of the Raman bands. Characterization of nanotube in adsorption gas has been studied by Monte Carlo and Langevin Dynamic Simulation (Monajjemi et al., 2008b). It is also important to investigate the effects of diameter on a SWCNT structure how the diameter depends on geometrical parameters such as the C-C bond lengths and some of the dihedral angles of SWCNTs.

For a better understanding of the physical and electronic properties of SWCNT, a challenging task in theoretical calculation is needed to specify the material properties because of the large size of the SWCNTs and their complicated (and size-dependent) electronic structure. Quantum calculation in prediction the properties of single-walled carbon nanotubes (SWCNTs) will be discussed.

2. Vibrational mode of SWCNT

Normal mode analysis has become one of the standard techniques in the study of the dynamics of nanotubes. It is primarily used for identifying and characterizing the slowest motions in a poly system, which are inaccessible by other methods. This text explains what normal mode analysis is and what one can do with it without going beyond its limit of validity. By definition, normal mode analysis is the study of harmonic potential wells by analytic means. The first section of this study will therefore deal with potential wells and harmonic approximations. This study is about normal mode approaches to different physical situations, and it discusses how useful information can be extracted from normal modes. Normalmode coordinates are obtained by a linear combination of Cartesian coordinates. Thus, there are no couplings in the kinetic part; that is, they diagonalize the kinetic energy as well the quadratic part of the potential energy operator. They include simultaneous motion of all atoms during the vibration, which leads to a natural description of molecular vibrations. Therefore, they are good candidates for representation of the molecular Hamiltonian. Since a transformation between different sets of coordinates is possible, the anharmonic terms can be calculated in one representation, and then transformed into another one.

2.1 Symmetry of SWCNT

Because a single carbon nanotube may be thought of as a graphene sheet rolled up to form a tube, carbon nanotubes should be expected to have many properties derived from the energy bands and lattice dynamics of graphite. For the very smallest tubule diameters, however, one might anticipate new effects stemming from the curvature of the tube wall and the closing of the graphene sheet into a cylinder. A method for identifying the Raman modes of single-wall carbon nanotubes (SWNT) based on the symmetry of the vibration modes has been widely used. The Raman intensity of each vibration mode varies with polarization direction, and the relationship can be expressed as analytical functions. Each Raman-active mode of SWNT can be distinguished from the group theory principle. The symmetry properties of periodic lattices of carbon nanotubes and the symmetry operations of chiral and achiral nanotubes (Damnjanović et al., 1999; Damnjanović et al., 2001; Alon, 2001, 2003) are usually described in terms of the group of the wavevector (Dresselhaus et al., 2006). However, since nanotubes can be viewed as quasi-1D systems, the line groups approach by Damnjanović et al. is suited to describe nanotube properties (Damnjanović et al., 1999).

As described earlier, the properties of nanotubes are determined by their diameter and chiral angle, both of which depend on n_1 and n_2. Typically, SWCNT is presented by a pair of integers (n_1, n_2). Its geometrical structure as shown in diagram can be represented in term of a chiral vector $\vec{C}$ on a two-dimensional sp²-carbon sheet where $\vec{C} = n_1\vec{a}_1 + n_2\vec{a}_2$ with integer n_1 and n_2. Here, $\vec{a}_1$ and $\vec{a}_2$ represent the unit vectors of the hexagonal graphene lattice. This sheet is then rolled up to a cylinder so that $\vec{C}$ becomes the circumference of the tube. The direction of the nanotube axis is naturally perpendicular to $\vec{C}$. The diameter, d, is simply the length of the chiral vector divided by ¼, and $d = \left(\sqrt{3}/\pi\right) a_{c-c}(n_1^2 + n_2^2 + n_1 n_2)^{1/2}$, where $a_{c\text{-}c}$ is the distance between neighbouring carbon atoms in the flat sheet. In turn, the chiral angle (θ) is given by $\tan^{-1}\left(\sqrt{3n}/(2n_2 + n_1)\right)$.

The translational period, *a,* is the shortest possible lattice vector along *z* direction. The translatory unit cell of a nanotube is a cylinder with a length in tube axis direction equal to the magnitude of the translation vector $\vec{T}$ as shown in Fig. 1 which can be calculated as following equation:

$$a = -\frac{2n_2 + n_1}{nR} a_1 + \frac{2n_1 + n_2}{nR} a_2$$

with

$$a = \mid a \mid = \frac{\sqrt{3(n_1^2 + n_2^2 + n_1 n_2)}}{nR} a_0$$

where *n* is the greatest common divisor of n_1 and n_2,

if $(n1 - n2)/3n \neq$ integer, then R = 1

if $(n1 - n2)/3n =$ integer, then R = 3

and $\vec{a}_1$ and $\vec{a}_2$ form an angle of 60° and their length is $\mid a_1 \mid = \mid a_2 \mid = a_0 = 2.461$ Å

Since the translational period, *a*, depends inversely on n and R the translation periodicity and thus the number of carbon atoms varies strongly for tubes with similar diameter. The number of graphene cells in the nanotube unit cell (n_c) obtained from:

$$n_c = 2q = 4\frac{n_1^2 + n_2^2 + n_1 n_2}{nR}$$

The groups of infinite line *L* are products *L* = *ZP*, where *P* is a point group and *Z* is the group of translations (screw axis, pure translations, and glide planes). Applying the above symmetry formulation to armchair ($n_1 = n_2$) and zigzag ($n_2 = 0$) nanotubes, such nanotubes with no caps have a isogonal point groups given by *q* (the number of graphene cells in the unit cell of the nanotubes) namely, D_{nd} when n is odd, D_{nh} when n is even, or *Dqh* = *D*2*nh* for achiral and *Dq* for chiral tubes. Whether the symmetry groups for armchair and zigzag tubules are taken to be D_{nd} or D_{nh}, the calculated vibrational frequencies will be the same; the symmetry assignments for these modes, however, will be different. It is, thus, expected that modes that are Raman or IR-active under D_{nd} (or D_{nh}) but are optically under *D*2*nh* will only show a weak activity resulting from the fact that the existence of caps lowers the symmetry that would exist for a nanotube of infinite length.

2.2 Active modes of Raman and IR

The phonon symmetries are found by decomposing the dynamical representation into its irreducible representations using symmetries of carbon and other nanotubes studied for line groups (Damnjanović et al., 1999). One direct set up of the dynamical representation from the atomic and vector representation is to use factor group analysis. A representation can be decomposed into the sum of its irreducible representations by the following formula

$$f_\alpha = \frac{1}{g}\sum_G \chi^{(\alpha)}(G) * \chi^{(\Gamma_{DG})}(G)$$

where $f\alpha$ is the appearance frequency of the irreducible representation α, *g* is the order of the symmetry group; the sum is over all symmetry operations *G*.

The Raman Γ_R and infrared active Γ_{IR} vibrations transform according to the representation of the second rank tensor and the vector representation, respectively (Damnjanović et al., 1983)

$\Gamma_R = [\Gamma_{vec} \otimes \Gamma_{vec}] = A_{1g} \oplus E_{1g} \oplus E_{2g} (\oplus A_{2g})$

$\Gamma_{IR} = \Gamma_{vec} = A_{2u} \oplus E_{1u}$

According to the symmetries of Raman-active modes (Pelletier, 1999) for the armchair carbon nanotube with the chair vector *(n1, n2)*, the point group for this kind nanotube belongs to D*n*h when *n* is even and its Raman-active modes are denoted by A1g + E1g + E2g. Three flavors of modes are longitudinal, transversal radial (orthogonal to tube surface) and transversal axial (parallel to tube surface). Satio et al. (Satio et al., 1998) pointed out that the low frequency A1g mode is a radial breathing mode and two high frequency is belong to Eg modes, E1g and E2g. E mode has the same displacement pattern with additional standing wave on the circumference.

2.3 Projection operators

The zigzag single-walled carbon nanotubes (SWCNTs) with (3,0), (4,0), and (5,0) structure were built using the tool in HyperChem7.0. The symmetries of the nanotube are D3d, D4d, and D5d respectively. Four different systems were studied in this work as follow: (1) gas-phase SWCNT, (2) SWCNT with 23 water molecules in the *a* x *b* x *c* box, (3) SWCNT with 23 methanol molecules in the *a* x *b* x *c* box, and (4) SWCNT with mixed solvent of water and methanol molecules in the *a* x *b* x *c* box. Energy minima of systems (2) – (4) were carried out by Metropolis Monte carlo (MC) calculation which generate random configurations in regions of space that make the important contributions to the calculation of thermodynamic averages. Then the ab initio and semiemperical with AM1 were used to optimize the structure of the nanotubes. All the normal mode frequencies and IR intensity were calculated using the optimized structures.

To find a function or the displacement pattern of eigenvectors transforming as a particular irreducible representation, the projection operators in group theory have been applied. Consider an arbitrary function *F*. This function can, in general, be expanded into several irreducible represent ations $F = \sum_\alpha \sum_n c_\alpha^n \zeta_\alpha^n$ where α labels the irreducible representations, c_α^n are the coefficients of the expansion, and the ζ_α^n are functions transforming according to the representation α. A projection operator defined by $P_{l(n)}^{(\beta)} = \frac{d_{(\beta)}}{g} \sum_G D_{\ln}^{(\beta)}(G)^* (G)$ applied to *F* picks out the symmetry adapted function $\zeta_l^{(\beta)}$. In equation d_β is the degeneracy of the irreducible representation β, g the order of the symmetry group, *G* are the symmetry operations, and $D_{ln}^{(\beta)}$ *ln* is the *ln*th element of the representation matrix $D^{(\beta)}$. From a given function, and its irreducible presentation, functions can be generating if that function has a "component" or a "non-zero projection" along the irreducible presentation of interest. This explains the name of "projector". As an example, if there is an orthonormal set *L*i of the function φ^i_1, φ^i_2,…,φ^i_{Li} which is used to form the i^{th} irreducible representation of a group by order *h*, for each operator, ***R***, in the group, by definition we can have:

$$\boldsymbol{R}\varphi^{i}_{t} = \Sigma s\varphi^{i}_{s}\, \Gamma(R)^{i}_{st} \tag{1}$$

By producting (1) in $[\Gamma(R)^{i}_{s't'}]^{*}$ and summing all over the symmetrical functions in the group we will have:

$$\Sigma_R[\Gamma(R)^{i}_{s't'}]^{*}\, \boldsymbol{R}\varphi^{i}_{t} = \Sigma_R\Sigma_s\, \Gamma\varphi^{i}_{s}\, \Gamma(R)^{i}_{st}\, \Gamma(R)^{\,i}_{s't'}]^{*} \tag{2}$$

Considering φ^{i}_{s} are functions independent from R, the right side of (2) can be written as: $\Sigma_s\varphi^{i}_{s}\ \Sigma_R\Gamma(R)^{i}_{st}\ [\Gamma(R)^{\,i}_{s't'}]^{*}$ So we have a series of Li terms and each of them are equal to a production of φ^{i}_{s} and a coefficient. These coefficients are following the orthogonality rule:

$$\Sigma_R\Gamma(R)^{i}_{st}\, [\Gamma(R)^{\,i}_{s't'}]^{*} = h/(L_iL_j)^{1/2}\, \delta_{ij}\, \delta_{ss'}\, \delta_{tt'} \tag{3}$$

By use of the eq.(3), the eq.(2) is simplified as follows:

$$\Sigma_R\Gamma(R)^{\,i}_{s't'}]^{*}\, \boldsymbol{R}\varphi^{i}_{t} = (h/L_j)\ \varphi^{i}_{s'}\, \delta_{ij}\, \delta_{tt'} \tag{4}$$

Now, by introducing

$$\boldsymbol{P^{j}_{s't'}} = L_j/h\ \Sigma_R\Gamma(R)^{i}_{st}\, [\Gamma(R)^{\,i}_{s't'}]^{*}\, \boldsymbol{R} \tag{5}$$

The eq.(4)gives the following form:

$$\boldsymbol{P^{j}_{s't'}}\varphi^{i}_{t} = \varphi^{i}_{s'}\, \delta_{ij}\, \delta_{tt'} \tag{6}$$

The $\boldsymbol{P^{j}_{s't'}}$ is call projection operator. The application of this operator on each φ^{i}_{t} is non-zero only when this function or some of its terms is a function of $\varphi^{i}_{s'}$. One of the most important application of this operator is projecting function φ^{i}_{t} from any function φ^{i}_{t}. In other words

$$\boldsymbol{P^{j}_{t't}}\varphi^{i}_{t} = \varphi^{i}_{t'}\, \delta_{ij}\, \delta_{tt'} \tag{7}$$

By use of the projection operator on the base of L_j diagonal elements of a matrix, we can have some φ^{i}_{t} functions, which are the bases for the j^{th} irreducible presentation (Wilson, et al., 1955)

2.4 The relation between projection and transfer operators

Assume that $\Gamma_k\ (p)_{\ ij}$ is the ij_{th} element of the matrix which shows the p^{th} operator ($\boldsymbol{O}p$) in k the k_{th} irreducible presentation. By this assumption the operator $\boldsymbol{O}_{\ k,\ ij}$ is defined as follows

$$\boldsymbol{O}_{\ k,ij} = L_k\ /\ h\ \Sigma_p\Gamma_k\ (p)^{*}_{\ ij}\, \boldsymbol{O}p \tag{8}$$

Where h is group order and L_k is the presentation dimension. If i = j these operators called Projection operators, $\boldsymbol{P}_{k,ii}$, in other words:

$$\boldsymbol{P}_{k,ij} = \boldsymbol{O}_{k,ii} \tag{9}$$

The non- diagonalized operators are called Transfer operators or shift operators,

$$\boldsymbol{T}_{k,ij} = \boldsymbol{O}_{k,ij}\,,\ i \neq j \tag{10}$$

In one-dimensional presentations $\boldsymbol{P}_{k,ij}$ and $\boldsymbol{O}_{k,ii}$ are the same and we have no $\boldsymbol{T}_{k,ij}$. With use of the above definitions, making the irreducible basis becomes possible in the following way:

At first the point group of the molecule is determined.Then the character of the system (Γ_{angles} or $\Gamma_{bonding}$) is calculated. By use of the standard reduce formulation these characters can be reduced to give the irreducible presentations:

$$n_{\Gamma} = 1/h \, \Sigma_g \, n_g \, \chi_R \, \chi_{\Gamma} \tag{11}$$

Where h is the order of the group, n_g is the number of the symmetry operation in the class of g, χ_R is the character of reducible presentation and χ_{Γ} is the character of irreducible presentation for the symmetric operations of class g. In this part there is a note about the reducing the $C_{\infty v}$ and $D_{\infty h}$ point groups. The method of reduce is a different from the normal method of reduce. For more information see from the references (Cotton, 1971; Schafer & Cyvrin, 1971; Strommen & Lippincott, 1972; Alvarino, 1978; Flurry, 1979; Strommen, 1979).
At the next step, the interested function is written by use of the projection operator. A set of the results gives the internal coordinate system for a given point group. There are several examples to illustrate this procedure in Table 1. The geometry and electrical properties of nanotube are very sensitive to dielectric constants. The normal modes also will be changed in the high dielectric constants. With the calculation of the normal modes using the U Matrix it is possible to get the F Matrix from the multiplication of frequency to the U Matrix. Solving the determination of F Matrix versus dielectric can be useful for understanding of the electrical behavior of nanotubes in the quantitative structure activity relationship (QSAR) studies. With use of the resulting coordinate system, the U Matrix (UMAT) can be written easily. These are matrices which perform the linear transformations on the internal coordinates sets (Alvarino & Chammoro, 1980).

2.5 Linear combination of primitive's harmonic vibrations and UMAT

The molecules and their internal coordinates of D4d have been given in Fig. 2. By following the above steps a complete set of the linear combinations and their normalization coefficients are achieved. The irreducible representations of the symmetry group are given by A and B. These data are given in Table 1. We use the application of projection operator method in finding the coordinate system, and by using it the U matrix is written and finally the frequencies and distributions of peak position are achieved. The (3, 0), (4, 0), (5, 0) zig-zag nanotubes were investigated. They have 66, 138, and 174 normal modes, respectively.

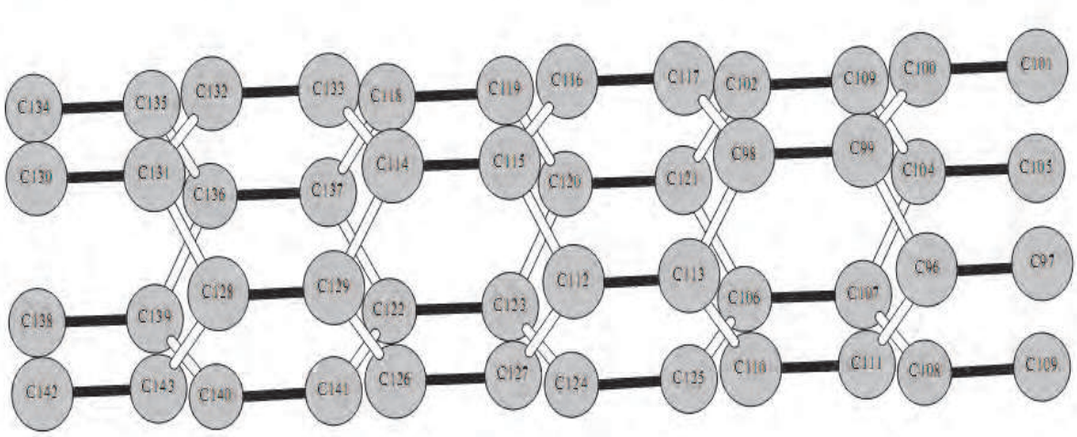

Fig. 2. The structure of (4, 0) nanotube in D_{4d} point group (Lee et al., 2009)

C_{2v}	E	C_2	n_v	n_d	Irreduced presentation	Primitives	Linear combination of primitives based on their symmetric A_1, A_2, B_1, B_2
Γ_1	3	1	1	3	$2A_1$ B_2	3	$S_1(A_1) = \frac{1}{\sqrt{2}}(R_1 - R_2)$, $S_2(B_2) = \frac{1}{\sqrt{2}}(R_1 - R_2)$, $S_3(A_1) = R_{31}$
Γ_2	3	1	1	3	$2A_1$ B_2	3	$S_4(A_1) = \frac{1}{\sqrt{2}}(R_4 - R_5)$, $S_5(B_2) = \frac{1}{\sqrt{2}}(R_4 - R_5)$, $S_6(A_1) = R_{32}$
Γ_3	3	1	1	3	$2A_1$ B_2	3	$S_7(A_1) = \frac{1}{\sqrt{2}}(R_{1'} - R_{2'})$, $S_8(B_2) = \frac{1}{\sqrt{2}}(R_{1'} - R_{2'})$, $S_9(A_1) = R_{33}$
Γ_4	3	1	1	3	$2A_1$ B_2	3	$S_{10}(A_1) = \frac{1}{\sqrt{2}}(R_{3'} - R_{4'})$, $S_{11}(B_2) = \frac{1}{\sqrt{2}}(R_{3'} - R_{4'})$, $S_{12}(A_1) = R_{34}$
Γ_5	3	1	1	3	$2A_1$ B_2	3	$S_{13}(A_1) = \frac{1}{\sqrt{2}}(R_{5'} - R_{6'})$, $S_{14}(B_2) = \frac{1}{\sqrt{2}}(R_{5'} - R_{6'})$, $S_{15}(A_1) = R_{35}$
Γ_6	3	1	1	3	$2A_1$ B_2	3	$S_{16}(A_1) = \frac{1}{\sqrt{2}}(R_{39} - R_{40})$, $S_{17}(B_2) = \frac{1}{\sqrt{2}}(R_{39} - R_{40})$, $S_{18}(A_1) = R_{36}$
Γ_7	14	2	2	2	$5A_1$ $3A_2$ $3B_1$ $3B_2$	14	$S_{19}(A_1) = \frac{1}{2}(R_1 - R_{1'} - R_2 + R_{2'})$, $S_{20}(A_2) = \frac{1}{2}(R_1 + R_{1'} - R_{2'} - R_{2'})$, $S_{21}^{(1)}(A_2) = \frac{1}{2}(R_{1'} - R_2 - R_1 - R_{2'})$, $S_{22}(A_1) = \frac{1}{\sqrt{2}}(R_1 - R_{1'})$, $S_{23}(A_1) = \frac{1}{\sqrt{2}}(R_2 - R_{2'})$, $S_{24}(A_1) = \frac{1}{\sqrt{2}}(R_{40} + R_{39})$, $S_{25}(B_2) = \frac{1}{\sqrt{2}}(R_{40} - R_{39})$, $S_{26}(A_1) = \frac{1}{\sqrt{2}}(R_{41} - R_{42})$, $S_{27}(B_2) = \frac{1}{\sqrt{2}}(R_{41} - R_{42})$, $S_{28}(A_1) = \frac{1}{2}(R_{39} - R_{39'} - R_{42} + R_{42'})$, $S_{29}(B_1) = \frac{1}{2}(R_{39} - R_{39'} + R_{42} - R_{42'})$, $S_{30}^{(1)}(B_1) = \frac{1}{2}(R_{39} + R_{39'} - R_{42} - R_{42'})$, $S_{31}(A_2) = \frac{1}{2}(R_{39} + R_{39'} - R_{42} - R_{42'})$
Γ_8	14	2	2	2	$5A_1$ $3A_2$ $3B_1$ $3B_2$	14	$S_{32}(A_1) = \frac{1}{2}(R_{3'} - R_{3} - R_{4'} + R_{4})$, $S_{33}(A_2) = \frac{1}{2}(R_{3'} + R_{4'} - R_{3} - R_{4})$, $S_{34}^{(1)}(A_2) = \frac{1}{2}(R_{3} + R_{4} - R_{3'} - R_{4'})$, $S_{35}(B_1) = \frac{1}{2}(R_{3} + R_{3'} - R_{4} - R_{4'})$, $S_{36}(A_1) = \frac{1}{\sqrt{2}}(R_{3} - R_{3'})$, $S_{37}(B_2) = \frac{1}{\sqrt{2}}(R_{4} - R_{4'})$, $S_{38}(A_1) = \frac{1}{\sqrt{2}}(R_{43} - R_{44})$, $S_{39}(B_2) = \frac{1}{\sqrt{2}}(R_{43} - R_{44})$, $S_{40}(A_1) = \frac{1}{\sqrt{2}}(R_{43} + R_{44})$, $S_{41}(B_2) = \frac{1}{\sqrt{2}}(R_{43} + R_{44})$, $S_{42}(A_1) = \frac{1}{2}(R_{43} - R_{43'} - R_{44} + R_{44'})$, $S_{43}(B_1) = \frac{1}{2}(R_{43} - R_{43'} + R_{44} - R_{44'})$, $S_{44}^{(1)}(B_1) = \frac{1}{2}(R_{43} + R_{43'} - R_{44} - R_{44'})$, $S_{45}(A_2) = \frac{1}{2}(R_{43} + R_{43'} - R_{44} - R_{44'})$

Γ_9	14	2	2	2	$5A_1$ $3A_2$ $3B_1$ $3B_2$	14	$S_{41}(A_1)=\frac{1}{2}(R_{51}+R_{55}+R_{58}+R_{54})$, $S_{44}(A_2)=\frac{1}{2}(R_{51}-R_{55}+R_{58}-R_{54})$, $S_{45}^{a}(A_2)=\frac{1}{2}(R_{56}+R_{57}-R_{52}-R_{53})$, $S_{46}(B_1)=\frac{1}{2}(R_{56}-R_{57}+R_{52}-R_{53})$, $S_{47}(A_1)=\frac{1}{\sqrt{2}}(R_{59}+R_{5,10})$, $S_{48}(B_2)=\frac{1}{\sqrt{2}}(R_{59}-R_{5,10})$, $S_{49}(A_1)=\frac{1}{\sqrt{2}}(R_{60}+R_{61})$, $S_{4,10}(B_2)=\frac{1}{\sqrt{2}}(R_{60}-R_{61})$, $S_{4,11}(A_1)=\frac{1}{\sqrt{2}}(R_{62}-R_{63})$, $S_{4,12}(B_2)=\frac{1}{\sqrt{2}}(R_{62}-R_{63})$, $S_{4,13}(A_1)=\frac{1}{2}(R_{64}+R_{67}+R_{68}+R_{65})$, $S_{4,14}(B_1)=\frac{1}{2}(R_{64}-R_{67}+R_{68}-R_{65})$, $S_{4,15}^{a}(B_1)=\frac{1}{2}(R_{66}+R_{69}-R_{70}-R_{71})$, $S_{4,15}(A_2)=\frac{1}{2}(R_{66}-R_{69}-R_{70}+R_{71})$
Γ_{10}	14	2	2	2	$5A_1$ $3A_2$ $3B_1$ $3B_2$	14	$S_{51}(A_1)=\frac{1}{2}(R_{13}+R_{17}+R_{18}+R_{15})$, $S_{52}(A_2)=\frac{1}{2}(R_{13}-R_{17}+R_{18}-R_{15})$, $S_{53}^{a}(A_2)=\frac{1}{2}(R_{14}+R_{19}-R_{20}-R_{16})$, $S_{54}(B_1)=\frac{1}{2}(R_{14}-R_{19}+R_{20}-R_{16})$, $S_{55}(A_1)=\frac{1}{\sqrt{2}}(R_{21}+R_{24})$, $S_{56}(B_2)=\frac{1}{\sqrt{2}}(R_{21}-R_{24})$, $S_{57}(A_1)=\frac{1}{\sqrt{2}}(R_{22}+R_{23})$, $S_{58}(B_2)=\frac{1}{\sqrt{2}}(R_{22}-R_{23})$, $S_{59}(A_1)=\frac{1}{\sqrt{2}}(R_{25}+R_{26})$, $S_{5,10}(B_2)=\frac{1}{\sqrt{2}}(R_{25}-R_{26})$, $S_{5,11}(A_1)=\frac{1}{2}(R_{27}+R_{30}+R_{31}+R_{28})$, $S_{5,12}(B_1)=\frac{1}{2}(R_{27}-R_{30}+R_{31}-R_{28})$, $S_{5,13}^{a}(B_1)=\frac{1}{2}(R_{29}+R_{32}-R_{33}-R_{34})$, $S_{5,13}(A_2)=\frac{1}{2}(R_{29}-R_{32}-R_{33}+R_{34})$

Table 1. The combination and their normalization coefficients of (3,0) nanotube in D3d point group (Lee et al., 2009)

The character of the system assigned by Γ was calculated from the character tables and the UMAT are written from the application of projection operator. Vibrational Calculation was carried out by the MOLVIB algorithms and by Hyper Chem. Calculation and a few sets of calculation were performed. Molecular motions can be assigned by the potential energy distribution (PED) analysis among internal coordinates by the method of the projection operator. There are good agreements between the most cases.

2.6 Normal mode dependence on dielectric

As can be inferred from Table 1 and the Fig. 3, 4, and 5, there are good agreements between the semi and Monte Carlo and even ab initio calculation. In Table 1 the various of intensity and frequency and potential energy from different methods are shown versus the inverse dielectric for some normal modes. From Fig. 3 we have two maximum for both of energy and frequency in the dielectric between 77.40 up to 70.42 and also the third maximum is located in the 61.76. This region range is considered to be the unstable geometry of nanotubes which are very sensitive to dielectric. After these range the frequency, intensity and energy goes toward a stable geometry which are not sensitive to dielectric. The same results are obtained in the insets Fig. B and C of Fig. 3 for D3d of normal mode 61 and 66 respectively. In the Fig 4, similar to normal mode 1 and 131 and 138 are shown with A, B, and C respectively for nano tube (4 0) in D4d point group, a common general behavior is observed in this nanotube as same as (3 0) nanotube, only with a shift in data, this shift is due to the difference between the geometrical structures of two nanotubes.

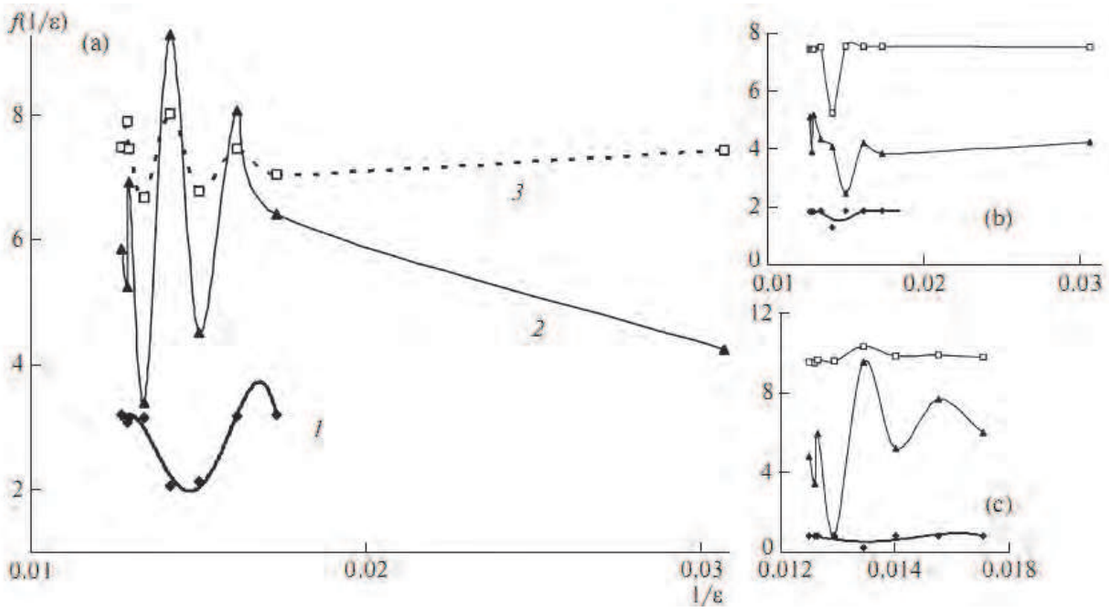

Fig. 3. The natural logarithms of the potential energy (1), intensity (2), and frequency (3) of three normal modes (a) 1, (b) 61, (c) 66 versus inverse of dielectric constant for nanotube (3, 0) with D3d point group by AM1 calculation (Lee et al., 2009)

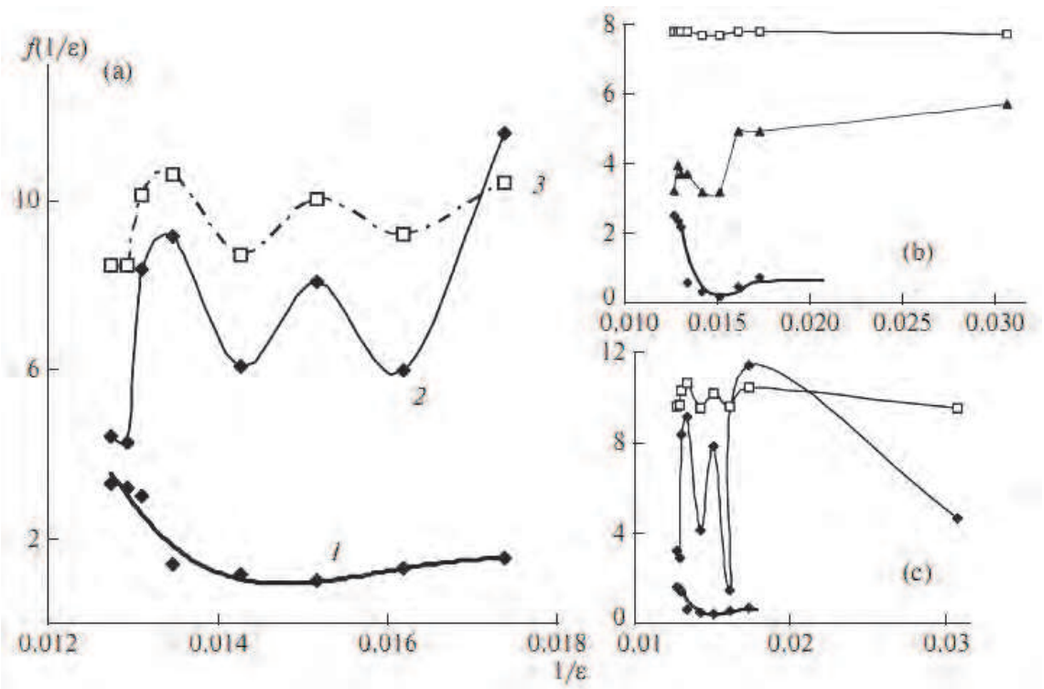

Fig. 4. The logarithms of the potential energy (1), intensity (2), and frequency (3) of three normal modes (a) 1, (b) 131, (c) 138 versus inverse of dielectric constant for nanotube (4, 0) with D4d point group by AM1 calculation (Lee et al., 2009)

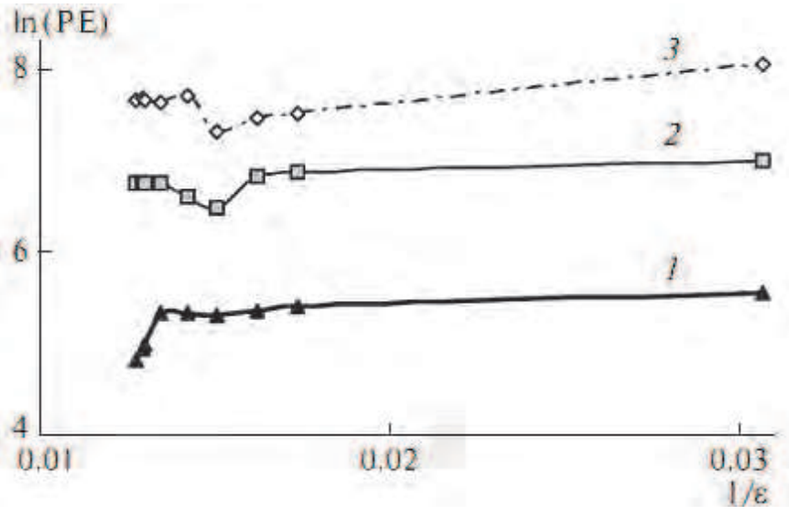

Fig. 5. The logarithms of the potential energy (PE) of three different zigzag nanotubes (1) D3d, (2) D4d, (3) D5d versus inverse of dielectric constant by MC simulations (Lee et al., 2009)

2.7 Potential energy dependence on the dielectrics of zigzag nanotubes

In Fig. 3 three line of potential energy for three nanotubes are shown by the Monte Carlo calculation versus dielectric constants. For D3d symmetric nanotube, the logarithm of potential energy increases as the dielectric constant reduces from 78.39 up to 76.10 while the D4d and D5d symmetries show an unchanged potential energy in this region. Beyond this point, the potential energy of D4d and D5d nanotubes drop and rise again to be in a new equilibrium, whereas the potential energy of the D3d mostly constant as the dielectric constant decreases. There are some changing in the energy in variable with the dielectrics above 60, and by decreasing the dielectrics the energy of three nanotubes goes toward constant variables. Similar trends between three figures and there are very good agreement with *ab initio* calculation in the Table 1.

3. Stability of SWCNTs: Solvents and temperature effects by molecular dynamics simulation and quantum mechanics calculations

Structural properties of solvents such as water, methanol, and ethanol surrounding single-walled carbon nanotube (SWCNT) and mixtures of them as well have an effects on the relative energies and dipole moment values. Because some of the physicochemical parameters are elated to structural properties of SWCNT, the different force fields can be examined to determine energy and other types of geometrical parameters, on the particular SWCNT. Because of the differences among force fields, the energy of a molecule calculated using two different force fields will not be the same. The structure of SWCNT as well as its dipole moments and relative energies has been studied by molecular dynamics simulation and quantum mechanics calculations (Monajjemi et al., 2010). The term "*Ab Initio*" is given to computations which are derived directly from theoretical principles, with no inclusion of experimental data. The most common type of ab initio calculation is called a Hartree-Fock (HF) calculation, in which the primary approximation is called the central field approximation. A method, which avoids making the HF mistakes in the first place, is called

Quantum Monte Carlo (QMC). There are several favors of QMC variational, diffusion, and Green's functions. These methods work with an explicitly correlated wave function and evaluate integrals numerically using a Monte Carlo integration. These calculations can be very time consuming, but they are probably the most accurate methods known today. In general, *ab initio* calculations give very good qualitative results and can give increasingly accurate quantitative results as the molecules in question become smaller (Monajjemi et al., 2008a). In general, there are three steps in carrying out any quantum mechanical calculation. First, prepare a molecule with an appropriate starting geometry. Second, choose a calculation method and its associated options. Third, choose the type of calculation with the relevant options and finally, analyze the results. We will give a short detail of computational method in the following section.

3.1 Molecular mechanics (Monte Carlo simulation)

The Metropolis implementation of the Monte Carlo algorithm has been developed by studying the equilibrium thermodynamics of many-body systems. Choosing small trial moves, the trajectories obtained applying this algorithmagree with those obtained by Langevin's dynamics (Tiana et al., 2007). This is understandable because the Monte Carlo simulations always detect the so-called “important phase space" regions which are of low energy (Liu & Monson, 2005). Because of imperfections of the force field, this lowest energy basin usually does not correspond to the native state in most cases, so the rank of native structure in those decoys produced by the force field itself is poor. In density function theory the exact exchange (HF) for a single determination is replaced by a more general expression of the exchange correlation functional, which can include terms accounting for both exchange energy and the electron correlation, which is omitted from HartreeFock theory:

$$E_{ks}=v+<hp>+1/2<P_j(\rho)>+E_{\chi(\rho)}+E_{C(\rho)}$$

where $E_{\chi(\rho)}$ is the exchange function and $E_{C(\rho)}$ is the correlation functional. The correlation function of Lee et al. includes both local and nonlocal terms (Lee et al., 1988).

3.2 Langevin dynamics (LD) simulation

The Langevin equation is a stochastic differential equation in which two force terms have been added to Newton's second law to approximate the effects of neglected degrees of freedom (Wang & Skeel, 2003). These simulations can be much faster than molecular dynamics. The molecular dynamics method is useful for calculating the time-dependent properties of an isolated molecule. However, more often, one is interested in the properties of a molecule that is interacting with other molecules.

3.3 Effect of differenct solvents of temperatures of SWCNTusing molecular dynamics simulation and quantum mechanics calculations

Difference in force field is illustrated by comparing the energy calculated by using force fields, MM+, Amber, and Bio+. The quantum mechanics (QM) calculations were carried out with the GAUSSIAN98 program based on HF/3-21G level. In the Gaussian program a simple approximation is used in which the volume of the solute is used to compute the radius of a cavity which forms the hypothetical surface of the molecule (Witanowski et al., 2002; Mora-Diez et al., 2006). The structures in gas phase and different solvent media such as

water, methanol, ethanol, and mixtures of them have been compared. The structure of SWCNT as well as its dipole moments and relative energies has been studied by molecular dynamics simulation and quantum mechanics calculations within the Onsager self-consistent reaction field (SCRF) model using a Hartree-Fock method (HF) at the HF/3-21G level and the structural stability of considered nanotube in different solvent media and temperature (between 309K and 327K) have been compared and analyzed.
Since the influence between a molecule in solution and its medium can describe most simply by using Onsager model, in this model we have assumed that the solute is placed in a spherical cavity inside the solvent. The latter is described as a homogeneous, polarizable medium of dielectric constant. We started our studies with HF/3-21G gas phase geometry and water, methanol and ethanol surrounding SWCNT and mixtures of them as well. The results obtained from Onsager model calculations are illustrated using the energy difference between these conformers which are quite sensitive to the polarity of the surrounding solvent. The solvent effect has been calculated using SCRF model. According to this method, the total energy of solute and solvent, which depends on the dielectric constant ε has been listed in Table 2.

Medium	Dielectric constant ΔE (Kcal/mol)	Temperature (K) 309	311	313	315	317	319	321	323	325	327
Gas phase	1	−0.1075	−0.1227	−0.0916	−0.1878	−0.1287	−0.1575	—	−0.0511	0	−0.1721
Water	78.39	−0.1929	−0.1965	−0.1573	0	—	−0.2629	−0.2316	−0.2517	—	—
Methanol	32.63	−0.0743	0	—	−0.0653	−0.1936	−0.0545	−0.1942	−0.0056	−0.0615	−0.0770
Ethanol	24.55	0	—	−0.0129	−0.0120	−0.0382	−0.0764	−0.0901	—	−0.0918	—
Water−Methanol	70.763	−0.0029	—	−0.0790	−0.0846	—	−0.0918	−0.0483	−0.0510	0	−0.0485
Water−Ethanol	69.416	−0.0840	−0.0852	−0.0442	−0.0215	—	−0.0276	−0.0890	0	−0.0144	−0.0610

Table 2. Theoretical relative energies at different temperature and dielectric constant

These energies have been compared with the gas phase total energy CNT at the HF/3-21G level of theory and different solvents, and the graph of energy values versus dielectric constant of different solvents has been displayed at considered temperatures in Fig. 6.

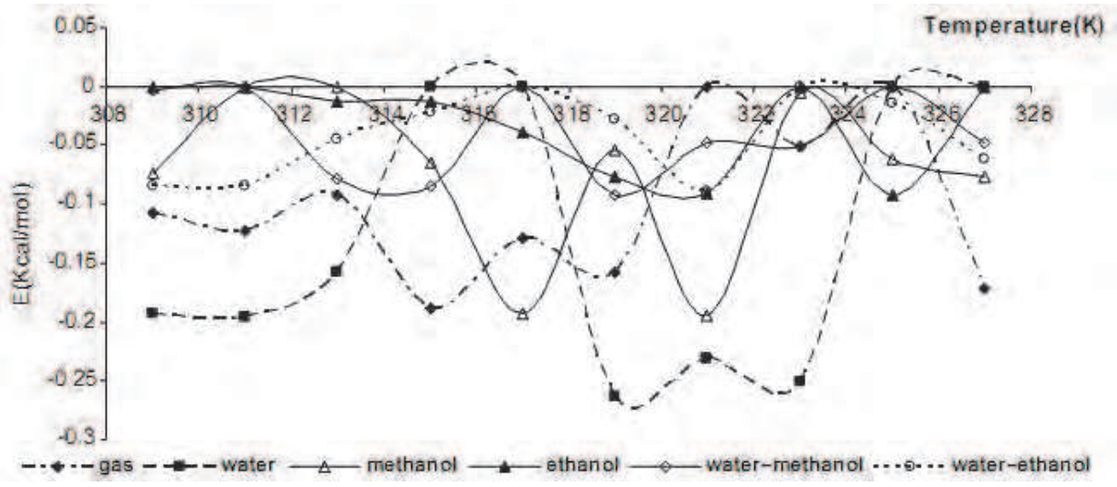

Fig. 6. The relative energy values at different temperatures in different solvents.

Since the solute dipole moment induces a dipole moment in opposite direction in the surrounding medium, polarization of the medium in turn polarizes the charge distribution in the solvent. The dipole moment value of SWCNT in different solvent media and at different temperatures has been reported in Table 3.

Medium	Temperature (K)									
Dielectric constant	309	311	313	315	317	319	321	323	325	327
Gas phase	14.8595	14.9783	15.8972	1.4569	12.7230	0.9106	—	15.1528	1.5045	0.7366
Water	1.3302	1.8910	1.0015	7.0286	—	0.7134	1.6209	0.9655	—	—
Methanol	1.4854	22.4244	—	9.5556	5.1790	9.4344	7.7342	21.3318	7.4751	7.2150
Ethanol	0.7029	—	2.4926	11.8624	14.9195	0.9389	0.9646	—	0.4796	—
Water−Methanol	12.4020	46.8625	4.4462	4.2048	—	4.8710	5.7352	5.9246	3.8414	6.1855
Water−Ethanol	0.8771	5.9677	6.3670	6.6015	—	3.8895	4.4362	6.4769	4.9592	5.8514

Table 3. Theoretical dipole moment values at different temperatures

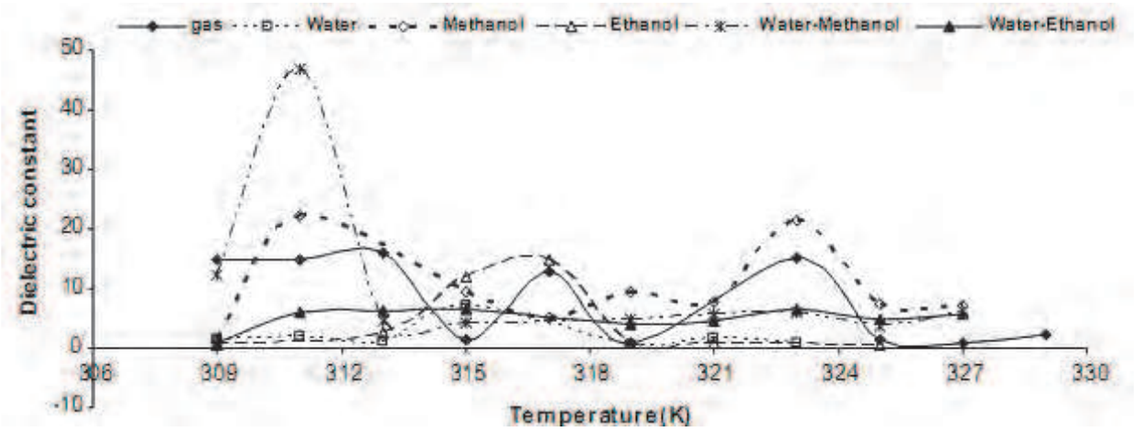

Fig. 7. The dipole moment values at different temperatures

One much more practical approach consists of calculating the molecular volume as defined through the contour of constant electron density, equating this (nonspherical) molecular volume to the radius of an ideally spherical cavity, and adding a constant increment for the closest possible approach of solvent molecules. This latter approach was used in Gaussian when the volume keyword was being used. In this work, we studied the structural properties of water, methanol, and ethanol surrounding SWCNT and mixtures of them as well as using molecular dynamics simulations. We used different force fields for determination of energy and other types of geometrical parameters, on the particular SWCNT. Because of the differences among force fields, the energy of a molecule calculated using two different force fields will not be the same. So, it is not reasonable to compare the energy of one molecule calculated with a particular force field with the energy of another molecule calculated using a different force field. In this study difference in force field illustrated by comparing the energy calculated by using force fields, MM+, AMBER, and BIO+. Theoretical energy values using difference force fields which are the combination of attraction van der Waals forces due to dipole-dipole interactions and empirical repulsive forces due to Pauli repulsion have been demonstrated in Table 4 and Fig. 8.

Medium	Dielectric constant	MM−	AMBER	BIO+
		E (kcal/mol)		
Gas phase	1	487.9812	382.4433	1628.176
Water	78.39	419.9189	316.7664	1560.24
Methanol	32.63	535.3614	431.2506	1533.685
Ethanol	24.55	468.4228	359.4595	1601.808
Water−Methanol	70.763	413.1738	309.1905	1484.31
Water−Ethanol	69.416	637.6032	539.6583	1476.198

Table 4. Theoretical energy values using different force fields

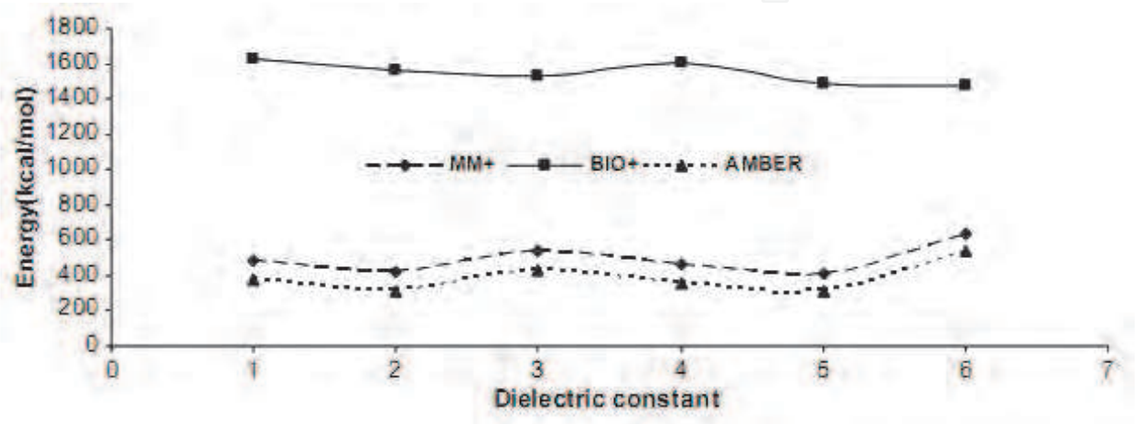

Fig. 8. The energy values using different force fields

The result of the calculated dipole moment, quadrupole moment, octapole moment, and hexadecapole moment values of SWCNT has been reported in Table 5, and optimized structures of nanotube in different media are shown in Fig. 9.

		Dipole moment			Quadrupole moment			Octapole moment					Hexadecapole moment								
		X	Y	Z	XX	YY	ZZ	XXX	YYY	ZZZ	XYY	XXY	XXXX	YYYY	ZZZZ	XXXY	XXXZ	YYYX	YYYZ	ZZZX	
Solvent	Temp	TOT			XY	XZ	YZ	XXZ	XZZ	YZZ	YYZ	XYZ	ZZZY	XXYY	XXZZ	YYZZ	XXYZ	YYXZ	ZZXY		ΔE
$SWCNT_{(10,0)}$ (4,7)	309	−14.6440	0.1709	−2.8154	−804.8781	−850.2825	−859.0581	−1865.5072	5.5459	−28.0528	−89.9615	8.0217	******	−15825.8820	−15280.2158	−74.7850	−1492.05	81.5585	6.0318	−117.1608	−0.107514
			14.8595		−0.5035	−18.7461	−1.1821	−163.5864	−88.7808	5.5858	−5.0588	−2.0505	−15.2039	−10782.5644	−19907.8851	−9110.2184	−84.6609	−28.5092	−1.7157		
	311	14.7152	0.1027	1.8413	−807.8251	−850.1959	−857.7486	1403.4845	5.8112	7.0879	88.5805	182.9025	******	−15894.6418	−15186.5538	−1724.0098	−1262.2806	−114.3129	−18.4200	−128.4575	−0.122794
			14.9783		−21.5888	−16.8081	−4.1513	155.8165	71.8007	5.8749	8.4020	17.0392	−94.7751	−10808.2405	−19811.4922	−8088.5585	−206.1877	−48.5857	−67.0681		
	313	15.4840	−2.4142	2.6682	−813.8514	−850.2292	−855.8187	1420.1102	−12.1769	16.5047	82.0814	−103.6747	******	−15171.8188	−15085.1858	1883.0053	−1002.4717	154.7071	25.2140	−107.2728	−0.091025
			15.6972		22.6096	−20.4078	2.4425	202.6841	68.7774	−7.0508	7.5074	−12.5116	−6.1269	−10883.0292	−19681.8544	−8041.8804	194.6506	−17.1804	52.2818		
	315	0.4056	−0.9083	1.0250	−712.1719	−859.4492	−855.5195	78.0914	1.6508	14.0220	97.5257	−66.2198	******	−15077.7207	−15084.1668	−70.2858	−257.0442	−92.8878	−14.0118	−24.0122	−0.187885
			1.4589		−1.4415	−8.4517	−0.8480	68.2204	−15.4389	−4.7577	2.5424	6.0305	5.1805	−10567.5789	−19102.4177	−8122.5845	−72.8018	14.6864	−6.8046		
	317	12.7077	0.5180	−0.8458	−797.7093	−852.5755	−857.7653	1225.0214	1.8741	−8.1095	18.4302	40.5788	******	−15492.8819	−15081.0940	−801.5745	630.3633	−98.1915	10.8582	184.3002	−0.12871
			12.7230		−0.5071	7.5095	1.2158	−51.5899	81.7003	−0.5721	1.8640	−11.6036	0.9070	−19451.0951	−19879.8155	−8102.7808	71.1309	−37.6227	−25.4519		
	319	−0.8855	−0.8136	0.1865	−715.8083	−860.1265	−856.3085	−16.8860	−5.4685	−1.7159	−17.5508	−26.1266	******	−15425.0187	−15140.8960	421.2191	−16.7040	51.4588	−58.8547	9.4804	−0.15756
			0.9105		6.2185	0.7334	−1.2094	6.8922	1.8009	−2.0058	1.5087	−0.8140	17.7448	−19585.7879	−19185.2741	−8108.0485	−92.0774	−10.7256	29.6024		
	321	—	—	—	—	—	—	—	—	—	—	—	—	—	—	—	—	—	—	—	—
			—		—	—	—	—	—	—	—	—	—	—	—	—	—	—	—		
	323	−15.0021	−1.6222	−0.3827	−807.7053	−856.2562	−851.9912	−1869.0078	−10.1028	2.4810	−86.1265	−146.9892	******	−15258.9407	−14950.8058	−2210.8053	−828.5021	−214.3513	1.2022	−17.4442	−0.051178
			15.1528		−28.7476	−11.4870	−5.5730	−21.9444	−40.9744	−4.1228	0.1815	−12.0892	−40.8885	−10815.1920	−19349.2708	−8088.8180	−317.6068	−118.3090	−68.0385		
	325	−0.1757	0.7800	1.2987	−780.6618	−855.4731	−859.3065	−80.5021	8.8081	22.7699	−21.7619	52.8099	******	−15418.2153	−15183.8142	−28.8290	−483.4387	80.5261	15.1284	52.2549	0
			1.5045		2.4855	−5.6029	2.6182	104.6224	14.7022	−1.6096	1.4874	−15.3525	11.3087	−19814.5094	−19508.0024	−8080.5406	219.0057	−79.8726	87.9432		
	327	0.0947	−0.6480	−0.3874	−718.5093	−860.0270	−855.8060	44.3072	−8.8020	−0.4140	−21.7775	−71.8008	******	−15533.6018	−15042.5782	430.0432	486.9275	70.5713	−11.8200	18.5049	−0.194847
			0.7866		6.1065	6.9554	2.2981	−11.6248	29.1555	−2.4015	−7.0050	30.6341	28.2809	−19600.5284	−19183.7105	−8074.8803	195.8413	28.7602	14.5447		
	329	−1.5082	1.0704	−1.1918	−792.6884	−857.8583	−857.8600	−167.2097	12.0277	−20.5520	−58.0183	54.0599	******	−15805.0207	−15283.1608	868.6320	265.3082	9.5175	−44.7107	55.0741	−0.172122
			2.0926		11.4800	8.2758	−6.4204	−80.1060	84.0920	5.8512	8.1285	−25.9273	−51.2774	−19520.5055	−19522.0786	−8114.1251	−451.9274	88.7111	105.8855		

		Dipole moment			Quadrupole moment			Octapole moment					Hexadecapole moment							
		X	Y	Z	XX	YY	ZZ	XXX	YYY	ZZZ	XYY	XXY	XXXX	YYYY	ZZZZ	XXXY	XXXZ	YYYX	YYYZ	ZZZX
Solvent	Temp		TOT		XY	XZ	YZ	XXZ	XZZ	YZZ	YYZ	XYZ	ZZZY	XXYY	XXZZ	YYZZ	XXYZ	YYXZ	ZZXY		ΔE
$SWCNT_{(12,6)}$-water	309	0.0078	0.2025	−0.0509	−721.6414	−659.6880	−659.2722	93.7872	−1.7243	−12.4079	20.6572	18.9168	******	−15454.1671	−15158.1740	400.8792	186.5951	48.5804	20.4502	84.2950	−0.192958
			1.3302		6.2040	3.0204	1.2292	−60.7160	0.7295	9.2513	1.1876	14.2028	18.6611	−10780.6831	−10808.8402	−5100.6283	44.4429	−51.0372	83.8705		
	311	0.6781	−1.6782	0.5537	−712.2610	−660.7997	−660.8692	78.8571	−14.1268	−8.0561	18.5044	−114.5149	******	−15816.8078	−14802.0649	787.0809	−887.9681	−69.7368	26.7012	−51.9885	−0.196564
			1.8010		7.4520	−3.9201	0.8210	40.5644	−5.6268	−8.7180	−1.7549	−10.8398	−7.1291	−10699.1198	−10648.7674	−5120.8105	188.7880	−1.1452	80.2818		
	313	−0.0173	−0.1928	−0.3526	−710.8840	−657.3922	−660.0078	−110.0308	−5.0247	−8.0210	1.8566	−27.0916	******	−15541.5077	−14954.6745	−105.4892	−416.0805	−61.2080	−27.1693	−64.7470	−0.157927
			1.0015		−2.8197	−4.0048	−0.4097	−27.0978	−18.2127	7.0109	−0.9826	18.9556	22.7802	−10624.5870	−10709.8499	−5092.8109	8.8751	4.6669	−8.9262		
	315	0.9644	−1.9958	0.0525	−919.6808	−659.4151	−662.6520	288.6782	−12.6057	45.8280	−27.8419	−169.0830	******	−15854.1349	−14858.1040	−118.2612	−99.1162	−26.8119	16.1684	−115.3540	0
			7.0286		−0.7842	−2.1383	1.7635	481.3953	65.4141	−8.6042	9.2140	−2.1691	−8.7709	−10571.4992	−10203.1009	−4986.5548	141.2782	85.4590	41.1064		
	317	—	—	—	—	—	—	—	—	—	—	—	—	—	—	—	—	—	—	—	—
			—		—	—	—	—	—	—	—	—	—	—	—	—	—	—	—		
	319	−0.8132	0.6143	0.1831	−717.1320	−658.6030	−658.0192	−47.9080	11.7478	6.1816	−19.9581	24.6070	******	−15548.7987	−14819.0157	406.7381	−226.1430	69.0447	15.9184	−55.9492	−0.202943
			0.7184		5.3825	−3.4315	0.9784	11.1880	18.0846	1.0844	−1.1261	15.6809	−14.5858	−10602.2749	−10508.6983	−5053.5839	135.0959	2.6647	20.2842		
	321	−1.5887	−0.4985	−0.1057	−721.3000	−662.6148	−655.8483	−119.1921	−5.9053	8.8843	−51.0617	−28.4512	******	−15812.4436	−15002.0102	−251.7614	270.4083	−81.7526	−7.2058	8.2568	−0.231667
			1.6209		−8.7784	3.0885	−2.7907	3.0626	88.8818	−6.1944	−9.7555	−15.1802	−15.8059	−20092.9270	−19247.4581	−5149.7668	−215.4586	29.8832	−22.2197		
	323	−0.0665	0.4220	0.8658	−721.0088	−657.0800	−663.4265	5.9553	2.1894	1.8781	0.1011	87.4186	******	−15580.2084	−14786.5079	564.9449	−516.1930	−10.3218	−34.8078	−20.5529	−0.251753
			0.9655		2.8852	−5.8053	−2.4870	64.6385	−19.6017	−5.5754	9.2236	18.8221	−4.0180	−10608.1419	−10830.8235	−5058.7565	−86.2293	−44.8580	−17.7865		
	325	—	—	—	—	—	—	—	—	—	—	—	—	—	—	—	—	—	—	—	—
			—		—	—	—	—	—	—	—	—	—	—	—	—	—	—	—		
	329	—	—	—	—	—	—	—	—	—	—	—	—	—	—	—	—	—	—	—	—
			—		—	—	—	—	—	—	—	—	—	—	—	—	—	—	—		

		Dipole moment			Quadrupole moment			Octapole moment					Hexadecapole moment							
		X	Y	Z	XX	YY	ZZ	XXX	YYY	ZZZ	XYY	XXY	XXXX	YYYY	ZZZZ	XXXY	XXXZ	YYYX	YYYZ	ZZZX
Solvent	Temp		TOT		XY	XZ	YZ	XXZ	XZZ	YZZ	YYZ	XYZ	ZZZY	XXYY	XXZZ	YYZZ	XXYZ	YYXZ	ZZXY		ΔE
$SWCNT_{(12,6)}$-(4,7)-ethanol	309	0.2801	0.2887	−0.0217	−720.7922	−657.5045	−659.7902	49.1533	8.1861	2.8580	4.7781	8.8844	******	−15479.6884	−15265.9007	859.4473	616.7403	109.2258	−16.4385	68.7184	0
			0.7029		11.1676	6.0212	−1.2966	−48.0874	6.0104	7.8095	−1.3545	−17.2971	−4.0074	−10529.0452	−10645.2758	−5184.8098	−108.3630	5.4027	7.0261		
	311	—	—	—	—	—	—	—	—	—	—	—	—	—	—	—	—	—	—	—	—
			—		—	—	—	—	—	—	—	—	—	—	—	—	—	—	—		
	313	2.1287	1.0149	−0.8078	−718.0002	−657.0558	−661.7489	191.5845	15.0457	−2.9289	6.4943	72.7805	******	−15581.7243	−15262.0879	71.5196	−378.9398	25.1173	−85.0108	−53.9576	−0.0129821
			2.4926		1.0357	−4.7548	−7.8447	−77.8805	29.7453	−2.4518	2.4926	64.2695	−52.0380	−10581.6480	−10851.1019	−5115.5588	−578.4797	13.0308	−4.2161		
	315	−10.8807	−2.6081	−4.0507	−776.4244	−657.7152	−656.2211	−485.0580	−11.5718	−83.1305	−65.8408	−249.7706	******	−15487.7085	−14808.7095	−2298.7485	−2482.9815	−225.0128	−94.8304	−195.5834	−0.012007
			11.8024		−28.5001	−80.0028	−9.0464	−287.4888	−53.0196	−15.2682	−18.2281	−83.1000	−7.0656	−10000.0024	−10706.3879	−5035.5149	−487.1965	−121.0555	−97.7227		
	317	−14.8819	0.5870	−1.5227	−649.1182	−654.8977	−659.1986	−703.9376	−8.0525	−6.8110	−88.9254	58.3050	******	−15468.8268	−14860.4576	128.5850	201.0876	20.0089	−80.1734	10.2732	−0.088293
			16.9195		8.0209	5.8111	−4.4158	−74.9155	−85.9965	5.7715	−0.2718	34.5488	−30.7181	−10295.7294	−10308.4680	−5030.0416	−846.1589	87.7840	0.7480		
	319	−0.0960	0.7055	0.5850	−724.1597	−660.2018	−661.8009	18.2858	18.0480	8.0618	−8.1416	1.4580	******	−15504.7425	−15141.2187	266.6092	−284.8215	62.2695	3.0252	−28.5701	−0.076492
			0.9389		5.2801	−4.1269	−0.6843	30.5798	11.4550	8.4970	−2.9818	−19.4796	1.2488	−10850.2985	−10912.8755	−5092.3333	−155.3072	−13.6530	53.0648		
	321	−0.4682	0.8802	0.0887	−712.4429	−662.8806	−655.8282	−28.7600	4.5630	2.8703	−24.1112	54.9080	******	−15545.0286	−14984.5692	−748.6216	188.7805	−17.5819	5.4303	26.7263	−0.09019
			0.9648		−7.4381	3.0080	0.7200	1.1257	15.7079	1.5852	−8.1452	−17.5552	1.1017	−10908.5852	−10938.4447	−5091.9980	49.8215	24.5089	−7.0894		
	323	—	—	—	—	—	—	—	—	—	—	—	—	—	—	—	—	—	—	—	—
			—		—	—	—	—	—	—	—	—	—	—	—	—	—	—	—		
	325	−0.0857	−0.1718	0.4492	−714.7845	−661.9806	−656.1977	−5.2923	−1.0334	−6.9482	11.8696	−32.7107	******	−15400.1851	−15082.4285	−808.9528	770.0901	−79.1779	32.1014	68.2614	−0.09184
			0.4796		−5.5091	10.1284	0.4297	25.0912	−21.5080	−1.0686	8.0053	8.1842	9.8388	−10930.0894	−10444.8108	−5078.5129	87.7034	25.6834	29.1105		
	327	—	—	—	—	—	—	—	—	—	—	—	—	—	—	—	—	—	—	—	—
			—		—	—	—	—	—	—	—	—	—	—	—	—	—	—	—		

		Dipole moment			Quadrupole moment			Octapole moment					Hexadecapole moment							
		X	Y	Z	XX	YY	ZZ	XXX	YYY	ZZZ	XYY	XXY	XXXX	YYYY	ZZZZ	XXXY	XXXZ	YYYX	YYYZ	ZZZX
Solvent	Temp		TOT		XY	XZ	YZ	XXZ	XZZ	YZZ	YYZ	XYZ	ZZZY	XXYY	XXZZ	YYZZ	XXYZ	YYXZ	ZZXY		ΔE
$SWCNT_{(12,6)}$-(4,7)-methanol	309	0.2825	−0.8428	1.2008	−783.4175	−661.9005	−658.1747	−24.7957	−7.4088	17.2260	88.8579	−46.9185	******	−15591.1987	−15174.4829	55.1877	758.0180	8.7870	21.6308	41.0697	−0.074869
			1.4854		−2.7756	7.8080	0.5457	43.8084	−88.7405	−0.4067	−2.1260	56.2727	58.2795	−10992.4746	−10545.9261	−5122.5088	230.7142	78.8713	−58.0477		
	311	−22.1601	−8.0275	−1.4895	−843.0728	−654.8508	−659.4412	−1803.7508	−27.4827	−5.1855	−89.9411	−287.1918	******	−15715.5048	−15302.5812	−1414.9994	−20.0895	−71.8516	4.7828	88.2617	0
			22.4244		−16.5498	−1.3655	1.4492	−108.5824	−107.1819	−6.7140	−7.1572	29.9161	25.1045	−20005.0502	−20270.8885	−5210.0858	95.4907	−11.0198	−118.2810		
	313	—	—	—	—	—	—	—	—	—	—	—	—	—	—	—	—	—	—	—	—
			—		—	—	—	—	—	—	—	—	—	—	—	—	—	—	—		
	315	−9.4004	0.6458	1.5806	−778.6807	−660.0144	−658.6832	−702.1821	−8.0824	12.0007	−56.2600	95.3777	******	−15540.1408	−15105.1051	594.0078	2745.0029	101.8607	49.5027	250.1460	−0.0658
			0.5556		6.2495	32.1031	4.2501	161.1667	−59.1013	−7.1102	12.1004	37.0965	6.7656	−20050.9552	−19875.0217	−5102.7071	344.1897	121.8207	−82.2689		
	317	−4.8084	1.0719	0.1802	−740.3056	−659.7450	−659.8531	−424.0047	29.1717	4.8840	−106.7746	119.1807	******	−15497.5748	−15379.6056	1290.1827	−485.7991	218.1838	−28.1675	−27.1485	−0.193681
			5.1790		14.8902	−6.8753	−9.2843	−20.2964	43.3589	−0.3222	7.1808	−1.1054	−39.6450	−19966.1746	−19883.2078	−5166.4385	−217.8272	48.7806	7.6704		
	319	−0.0138	2.8724	−1.4509	−768.9798	−660.5028	−654.0860	−807.1521	82.6762	−4.4180	−108.8003	167.7784	******	−15548.6875	−15287.9881	1542.6574	−730.1954	249.7533	−8.6915	−20.0014	−0.054581
			9.4344		19.1250	−9.8784	0.9304	−97.8407	6.8126	0.5194	−7.2767	15.1337	29.8073	−20156.8186	−19448.6015	−5128.8066	19.8514	−20.3876	18.3278		
	321	7.5748	−0.2098	−1.5479	−752.0855	−657.0198	−662.1121	648.0518	−7.0026	−22.1078	42.5120	−11.0003	******	−15516.5820	−15363.2650	−185.2120	1811.5929	−76.0007	−30.6852	186.9994	−0.194206
			7.7942		−8.7412	14.1483	−4.4097	−118.0825	54.6421	−8.7733	−5.1812	39.0404	−9.9496	−19654.8508	−20027.7955	−5149.8249	−418.8877	89.5004	52.1312		
	323	21.2212	1.0805	0.8660	−844.7077	−660.0454	−653.9360	1778.9615	−12.7277	9.1955	108.5071	143.1008	******	−15585.2568	−15158.0990	−796.8709	−830.9301	14.7980	−29.8364	−120.8203	−0.005656
			21.3318		−12.1309	−18.0211	−4.4294	56.7607	98.1184	9.8276	1.0805	1.5679	−82.8286	−20894.1003	−19800.3528	−5066.4851	−976.2565	−47.0784	−24.0052		
	325	−7.0492	−1.0855	1.5921	−752.0485	−662.1841	−658.5841	−544.6619	−18.6946	2.9082	−80.8045	−106.5488	******	−15597.9551	−15297.5060	−1180.3778	2293.8445	−192.0550	43.8185	94.9529	−0.061553
			7.4751		−15.5308	28.4839	5.3891	167.1891	−22.5081	−7.3815	5.8047	33.2038	32.0312	−20164.9858	−19771.1511	−5142.8851	445.0417	200.5094	−51.8619		
	327	−7.0087	1.5284	0.7788	−752.1815	−662.1982	−654.1601	−715.1820	19.4842	2.9492	−86.0888	121.9088	******	−15647.8111	−15124.5612	1810.6884	−511.0312	202.0872	−19.4090	−99.7850	−0.077016
			7.2150		16.7021	−7.6145	−1.8681	97.4825	−14.4841	−0.0950	3.9120	−16.8110	−16.4849	−20224.8224	−19477.8204	−5140.7928	−182.0415	44.8731	6.2946		

		Dipole moment			Quadrupole moment			Octapole moment					Hexadecapole moment								
		X	Y	Z	XX	YY	ZZ	XXX	YYY	ZZZ	XYY	XXY	XXXX	YYYY	ZZZZ	XXXY	XXXZ	YYYX	YYYZ	ZZZX	
Solvent	Temp	TOT			XY	XZ	YZ	XXZ	XZZ	YZZ	YYZ	XYZ	ZZZY	XXYY	XXZZ	YYZZ	XXYZ	YYXZ	ZZXY		ΔE
$SWCNT_{(12,7}$ (4,7)-water – ethanol	309	0.6751	0.4929	−0.2656	−712.5204	−655.2920	−663.5865	88.9541	4.7226	−8.7045	29.8280	−1.0083	******	−15425.2290	−14705.8716	−822.9457	−835.2780	−91.5718	7.9254	−2.6228	−0.064098
			0.8771		−5.5049	−5.4217	1.2912	−2.5657	−24.0551	8.8002	4.0472	−19.9880	13.0804	−19563.9745	−19988.9291	−5024.1302	129.1434	−68.4288	−24.6220		
	311	−5.5825	−2.0302	0.0805	−782.2581	−661.7001	−664.7473	−456.1802	−7.5924	15.3594	84.4029	−116.0547	******	−16609.5859	−15464.7497	−649.8821	2036.5301	−60.5729	0.8479	821.7151	−0.085221
			5.9677		−10.1584	24.7073	4.5949	122.0001	−94.0670	−16.4499	8.4874	21.2429	75.1825	−19746.7585	−19088.7274	−5854.2888	308.8526	21.0294	−153.9256		
	313	−5.7577	−1.9182	1.9257	−729.0999	−661.8659	−666.4156	−470.8702	−11.8652	28.9506	−2.4557	−122.0853	******	−16386.2052	−15508.7053	−453.8679	1097.9675	−8.2973	24.1864	154.0812	−0.044280
			6.3670		−2.8586	12.3061	3.8830	182.2285	−51.1772	−12.2148	0.8418	27.0542	31.2700	−19652.9260	−19877.7251	−5327.7026	296.6603	35.0241	−140.9214		
	315	−6.0967	−1.5304	2.0100	−730.6855	−659.4816	−667.9510	−456.8056	−18.0449	33.0751	16.8187	−84.8076	******	−16745.0814	−15503.9051	156.0592	884.4741	84.1865	1.8405	124.5123	−0.021558
			6.6015		0.4228	10.4290	3.6773	180.5086	−74.0004	−13.0272	−5.2588	47.5480	35.8160	−19587.8032	−19918.5923	−5376.9268	271.6607	19.4847	−126.5068		
	317	—	—	—	—	—	—	—	—	—	—	—	—	—	—	—	—	—	—	—	
			—		—	—	—	—	—	—	—	—	—	—	—	—	—	—	—		
	319	5.6530	−0.5571	−1.2138	−741.7181	−658.7082	−669.9092	380.4041	−12.0154	−31.1419	14.1080	1.7784	******	−16702.4808	−15507.5685	482.0524	930.5850	41.7507	−24.9775	177.1722	−0.027679
			8.8805		7.8311	10.2308	−2.1702	−120.2621	23.0542	−8.8039	4.2285	9.7827	−18.1290	−19497.3808	−20015.8812	−5308.4028	−136.5817	−31.1998	104.7985		
	321	−6.2797	−1.1785	0.1829	−734.0280	−658.0000	−666.2975	−458.0937	−6.9988	5.5957	−11.9927	−56.8552	******	−16826.9490	−15529.4392	−1114.0878	2005.0098	−158.1294	18.1705	328.0808	−0.080011
			4.4382		−16.3884	25.8878	8.8309	28.4876	−28.4055	−17.0712	8.9808	35.2403	11.8085	−19450.6580	−19665.0505	−5406.7469	225.7249	24.2015	−159.0748		
	323	−6.4297	0.2887	0.7480	−748.4172	−661.1047	−664.0051	−585.8458	2.7830	16.7089	−18.4097	88.4390	******	−16628.9472	−15714.0922	−1103.8838	851.8480	−208.8875	16.9704	89.6261	0
			6.4769		−17.1796	7.9433	4.8720	84.8085	−51.1356	−15.8860	0.1690	35.7176	52.8093	−19489.8441	−19507.8702	−5415.8307	295.9076	8.0434	−139.6450		
	325	−6.4197	1.7130	−1.4580	−743.2502	−657.5881	−668.5018	−499.0851	25.7112	−15.4201	−26.6555	77.1864	******	−16554.2859	−15714.5875	885.0122	−1184.6577	109.8558	82.8134	−188.7083	−0.014485
			4.9502		18.8487	−18.6525	4.4219	−128.3076	−25.6590	18.1474	−4.8096	26.9011	27.8881	−19208.1295	−19788.0291	−5399.1027	355.0758	−62.9532	178.0209		
	327	5.7009	0.9564	0.0078	−740.9573	−661.7147	−664.2185	480.0343	7.2989	12.6965	26.5207	72.6647	******	−16680.0392	−15699.1424	−959.2686	−1609.9506	−144.1439	−42.4570	−280.6280	−0.061018
			5.8514		−13.8708	−20.7771	−6.5811	111.0938	37.0460	11.9501	1.3096	37.0988	−72.1748	−19411.1850	−19505.5483	−5402.5271	−462.1145	−20.2798	−122.2988		

		Dipole moment			Quadrupole moment			Octapole moment					Hexadecapole moment								
		X	Y	Z	XX	YY	ZZ	XXX	YYY	ZZZ	XYY	XXY	XXXX	YYYY	ZZZZ	XXXY	XXXZ	YYYX	YYYZ	ZZZX	
Solvent	Temp	TOT			XY	XZ	YZ	XXZ	XZZ	YZZ	YYZ	XYZ	ZZZY	XXYY	XXZZ	YYZZ	XXYZ	YYXZ	ZZXY		ΔE
$SWCNT_{(12,}$ (4,7)-water – methanol	309	−11.3885	2.5802	4.1724	−701.4385	−658.0008	−656.6402	−1159.8492	14.7805	41.5895	−60.4705	217.5504	******	−15685.9819	−14508.9912	1975.8405	8524.4047	105.1303	−88.2100	847.8424	−0.002968
			12.4020		22.0780	42.5160	−4.0800	330.9982	−86.8268	1.2714	8.5941	−72.4616	9.0052	−20204.2667	−19726.7142	−5022.9658	−880.4378	58.5911	78.8472		
	311	−8.7794	−0.6031	−46.0288	−629.0088	−687.5810	−681.0955	621.0819	−1.8708	−1430.9166	125.4008	6.3108	******	−15719.3000	−28256.2842	820.4061	−8014.6728	110.0702	16.5485	−686.7580	−85.7480
			46.8925		2.6402	−176.7508	−2.7102	−657.4983	−879.5485	−89.4302	−16.5889	−67.7183	−92.6187	−19483.7004	−22405.5998	−5925.4211	283.8390	−209.8270	−84.6808		
	313	3.9552	−0.9676	1.7856	−749.1780	−662.2205	−661.3851	399.3294	−18.5843	−8.8486	56.0750	−92.1804	******	−16525.7085	−14620.9458	758.0083	−856.6283	45.7953	65.1172	−65.0932	−0.070089
			44462		8.6286	−10.6025	0.5805	181.0510	−5.6580	−8.8670	22.5080	−85.2857	56.0878	−20370.5992	−19925.2887	−5008.5564	410.0442	−108.0026	162.6425		
	315	4.0448	0.4069	1.0750	−736.7582	−662.0093	−660.2584	298.1491	4.5389	−14.7818	43.8880	−1.5896	******	−15967.9270	−14802.8729	598.7184	−905.9110	70.3187	9.7987	−46.8671	−0.084662
			4.2048		6.5857	−7.9183	3.2949	118.5303	28.2924	−0.8805	15.9015	−88.8850	48.1870	−20208.1694	−19745.6228	−5068.8518	387.7029	−84.1165	123.7279		
	317	—	—	—	—	—	—	—	—	—	—	—	—	—	—	—	—	—	—	—	—
			—		—	—	—	—	—	—	—	—	—	—	—	—	—	—	—		
	319	4.7164	−0.0075	1.2171	−745.6118	−662.4589	−657.9540	471.1509	−7.2490	−5.7600	88.8019	−2.0844	******	−15650.7850	−14882.9191	1509.8402	−1293.7610	167.2057	24.8207	−71.3886	−0.091821
			4.8710		19.1851	−15.4781	0.9449	128.4669	26.0887	−5.6816	15.2807	−57.9027	8.6201	−20382.0660	−19760.1130	−5081.4305	97.2160	−181.0272	171.1821		
	321	−5.0672	−1.5077	−2.1595	−743.1684	−662.5592	−660.4124	−444.2160	−16.8092	−15.2040	−35.7271	−120.9415	******	−15162.1831	−14457.6679	−1084.1554	−1152.8088	−195.8307	−26.0555	−83.2703	−0.048831
			5.7552		−14.8038	−15.2385	−2.0273	−140.6448	−85.4025	−11.9477	−14.6877	−66.0855	−14.7093	−20416.8795	−19849.4300	−5107.8802	−166.1022	−183.8515	−134.0981		
	323	−5.8387	0.7194	0.7425	−740.5808	−662.0042	−661.2422	−585.2028	5.8709	−6.4880	−66.5705	57.8197	******	−16088.5196	−14884.6212	1841.1430	1672.5287	207.0850	−76.4301	95.1824	−0.051009
			5.9245		21.7821	21.3857	−7.5498	105.8218	−27.4808	14.7270v	11.3174	−58.9470	−35.1778	−20404.8091	−19718.2706	−5098.5996	−505.8721	181.5597	158.6705		
	325	−0.0894	−1.8057	−3.1913	−758.4672	−661.0518	−661.8919	−8.8386	−0.0721	−20.1092	−28.1870	−151.3141	******	−15709.0800	−14843.8708	−1383.8534	−1807.0990	−188.2195	−17.7332	−163.1191	0
			8.8414		−17.4702	−20.8205	−0.9708	−251.5518	−7.4980	−20.8805	−20.0040	−79.6055	−9.5896	−20302.6052	−19999.3695	−5111.5054	−59.5080	−184.8812	−116.9775		
	327	5.5830	−0.8291	1.2907	−750.2504	−659.0515	−659.0877	515.0852	−29.5770	2.8401	54.7252	−102.0588	******	−15794.1671	−14524.9496	1899.0896	−1780.3051	255.4472	67.2278	−142.0949	−0.048575
			8.1855		24.3467	−25.2385	8.4008	101.5817	16.9284	−12.7722	10.3198	−24.4762	61.8170	−20121.0397	−19819.0530	−5071.2223	628.7498	−184.1491	177.3505		

Table 5. The calculated dipole moment, quadrupole moment, octapole moment, and hexadecapole moment values of SWCNT

4. NMR and IR theoretical study on the interaction of doping metal with carbon nanotube (CNT)

Numerous electrical measurements on SWCNT ensembles have revealed that chemical doping by donors (Li, K, Cs, or Rb) or acceptors (Br_2, I_2, or acids) decreases the room temperature electrical resistance by up to two orders of magnitude at saturation doping (Kaaoui et al., 1999; Coluci et al. 2006). The important problem is metals passing through cells membrane. Because, there are barriers for them passing through protein canals in cells membrane. Additionally, upon interaction, changes in activity, stability, and solubility ions compatibility may occur in cells. A lot of studies are for replacing protein canals into cells membrane for passing proteins, drug and ions of metal. Therefore the presence of the SWCNT and its consequences to the biological activity of ions metal are of high impact in

the development of biosensors, immunoassays and drug delivery systems (Zhang et al., 2005; Ganjali et al., 2006). This work, we used armchair carbon nanotube (5, 5) and (6, 6). Indeed, vibrational frequencies of finite-length carbon nanotubes were recently examined (Tagmatarchris & Prato, 2004) and another result of 319.9 cm^{-1} is consistent with oscillations along the radial directions (radial modes), although it cannot be assessed accurately due to the sensitivity to the number of rings (Yumura et al., 2005). We suggest that SWCNT intercalate into cells membrane replacing protein canals and are studying passing metal ions (Na, Mg, Al, and Si) in length of SWCNT by Quantum Mechanics (QM).

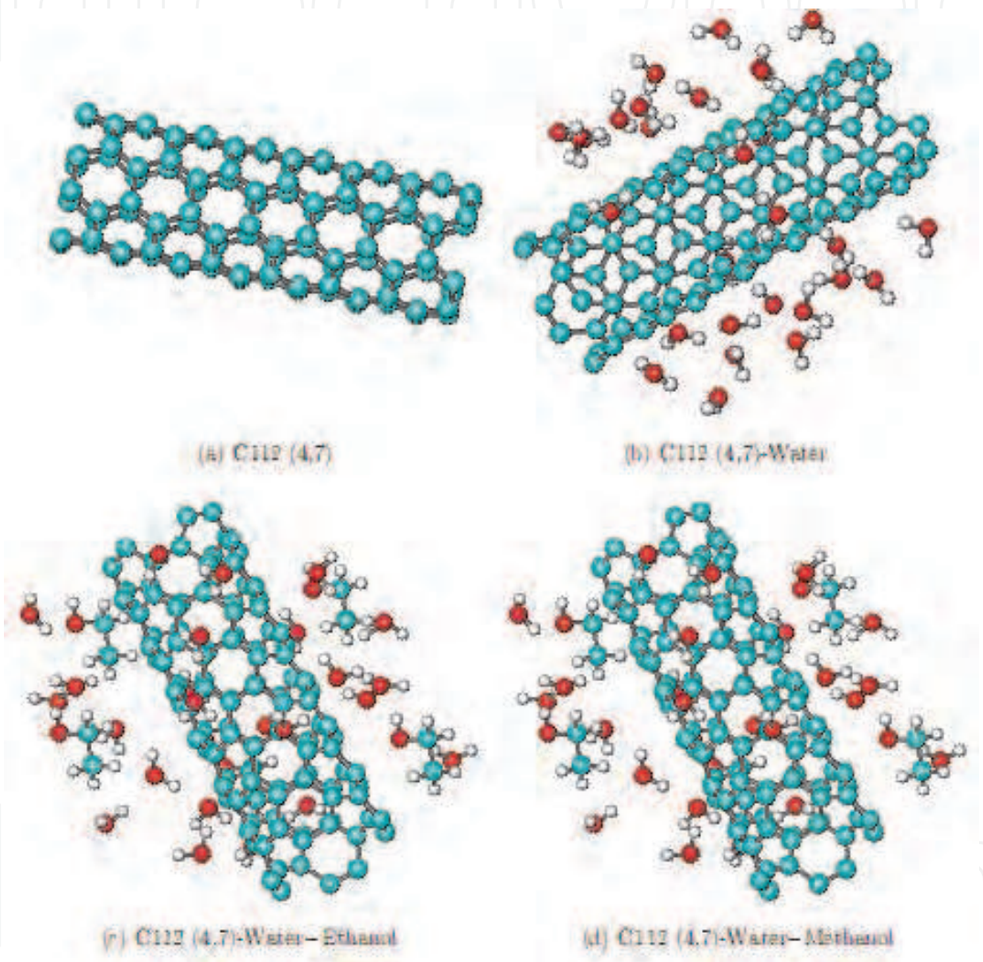

Fig. 9. Optimized structures of nanotube in different media

4.1 Computational details

The geometry optimizations were performed using an all-electron linear combination of atomic orbitals Hatree–Fock (HF) and density functional theory (DFT) calculations using the Gaussian A7 package. SWCNTs (100–120) from kind of armchair carbon nanotubes (5, 5) and (6, 6) show in Fig. 10. We are interested in the structural features of single-walled carbon nanotube (SWCNT) in the ground state an atomic and amino acids (His and Ser). In HF theory the energy has from:

$$E_{ks}=v+<hp>+1/2<P_j(\rho)>-1/2<P_k(\rho)>$$

where v is the nuclear repulsion energy, ρ is the density matrix, ⟨*hp*⟩ is the one electron (kinetic plus potential energy). 1/2 ⟨$P_j(\rho)$⟩ is the classical coulomb repulsion of the electrons and –1/2 ⟨$P_k(\rho)$⟩ is the exchange energy resulting from the quantum (fermions) nature of electrons.

In density function theory the exact exchange (HF) for a single determinant is replaced by a more general expression the exchange correlation functional, which can include terms accounting for both exchange energy and the electron correlation, which is omitted from Hartree–Fock theory:

$$E_{ks}=v+<hp>+1/2<P_j(\rho)>+E_{\chi(\rho)}+E_{C(\rho)}$$

where, $E_{\chi(\rho)}$ is the exchange function and $E_{C(\rho)}$ is the correlation functional. The correlation function of Lee, Yang, and Parr is includes both local and non-local term (Kar et al., 2006). The optimizations of solids are carried out including exchange and correlation contributions using Becks three parameters hybrid and Lee–Yang–Parr (LYP) correlation [B3LYP]; including both local and non-local terms with the program Gaussian A7 package (Lee et al., 1988; Becke, 1993; Becke, 1997).

Compared to Raman spectroscopy, much less information about the vibration properties of carbon nanotubes can be gained from IR spectra. This limitation mainly results from the strong absorption of SWCNTs in the IR range. Accurate predictions of molecular response properties to external fields are of general significance in various areas of chemical physics. This especially refers to the second-order magnetic response properties (NMR), since the magnetic resonance based techniques have gained substantial importance in chemistry and biochemistry that NMR data shown with two parameters isotropic (σ_{iso}) and an isotropic (σ_{aniso}) shielding.

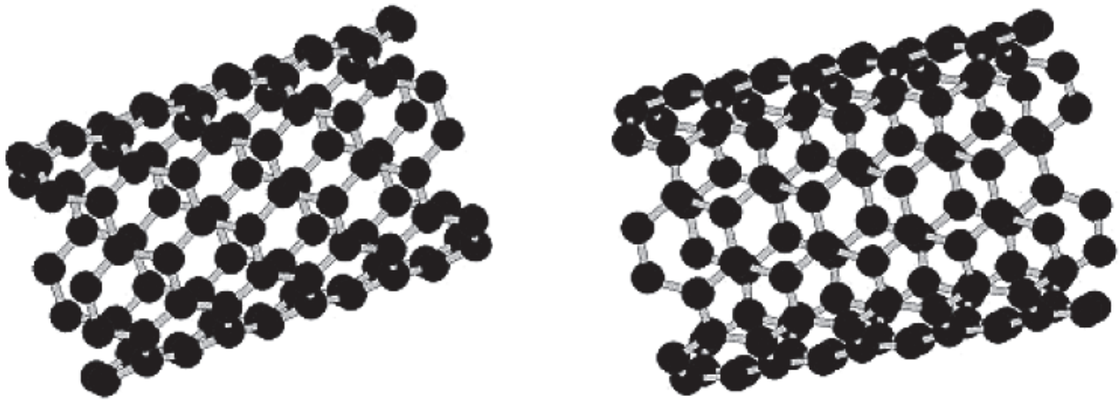

Fig. 10. The optimized configuration Side-view SWCNT: C_{100} (a) and C_{120} (b)

4.2 Interaction of Na, Mg, Al, Si with Carbon Nanotube (CNT): NMR and IR Study

The B3LYP and HF by 6–31G and 6–31G* calculaion for the molecular SWCNT models with Na, Mg, Al, and Si considered were validated by the calculated 13C and 1H NMR shifts and thermodynamic properties of an open-ended SWCNT (5, 5) and (6, 6) molecular systems (Monajjemi et al., 2009). The total energy (Etotal) of this interaction is listed in Table 6, which the Etotal increase to converge with an increasing carbon number.

Energy total (Hartree)		Na				Mg		Al		Si	
		HF	B3LYP	HF	B3LYP	HF	B3LYP	HF	B3LYP	HF	B3LYP
C_{100}	6-31G	–2241.98	–2256.53	–2401.83	–2416.63	–2438.87	–2453.67	–2480.80	–2495.72	–2527.27	–2542.30
(5,5)	6-31G*	–2269.16	–2284.21	–2430.75	–2446.16	–2468.15	–2483.58	–2510.66	–2526.16	–2557.67	–2573.29
C_{120}	6-31G	–2990.32	–3009.391	–3150.15	–3169.61	–3187.08	–3206.55	–3229.18	–3248.72	–3275.58	–3295.37
(6,6)	6-31G*	–3026.37	–3046.26	–3188.02	–3208.34	–3225.34	–3245.70	–3267.95	–3288.37	–3315.00	–3335.57

Table 6. The total energy calculated in various basis set at HF & B3LYP for SWCNTs (5,5) and (6,6) with ions metal Na, Mg, Al and Si

In this study the metals on the center of a hexagon (HC) and muse are related to competitive interactions between ions metal and SWCNTs. The structural electronic and magnetic properties have been investigated. The most stable configuration for Si adsorbed on SWCNTs is also at the (HC) site at competitive another atoms of SWCNT because the electro negativity is the most great. The calculated amounts of Dipole, Quadrupole, Octapole, and Hexa-decapole moments at the HF and B3LYP levels in various basis set are given in Table 7. Hybridizing Coefficient is different in various methods and basis set.

Calculations of the NMR shifts with the magnetic field perturbation method of GIAO (gauge in dependent atomic orbital) incorporated with the program Gaussian A7 package. The results of the calculations for the carbon nearest neighbors' atoms in SWCNTs are presented in Table 7. The calculated magnetic shielding in Figs. 11, 12 was converted into σ_{iso}, σ_{aniso} chemical shifts by 13C absolute shielding in SWCNT (5, 5). They are worth noting that the last approach leads to a substantial improvement in the calculated magnetic properties. Regarding the method for achievement of gauge invariance for the present case, at the B3LYP and HF levels on the other hand at the hybrid B3LYP level, GIAO is found to be slightly superior. The calculated infrared is for C100 at HF/6–31G with Na, Mg, Al, and Si. They showed in Table 2. The properties thermodynamic are decrease with increase electro negativity atoms.

	Cv_{th} (cal/mol)	S_{th} (cal/mol)	H_{th} (cal/mol)	G_{th} (cal/mol)	E_{th} (cal/mol)
$SWCNT_{100}$(5.5)	104.25	146.61	245.64	201.93	245.05
$SWCNT_{100}$-Na	103.13	139.32	262.12	220.60	261.68
$SWCNT_{100}$-Mg	103.44	138.53	255.49	214.21	255.04
$SWCNT_{100}$-Al	105.85	142.81	247.06	204.50	246.61
$SWCNT_{100}$-Si	105.58	143.55	243.11	200.33	242.65

Table 7. Calculated thermal energy, thermal enthalpy, total enthalpy, thermal entropy, thermal Gibbs free energy, Gibbs free energy, and heat capacity by IR-HF/6-31G

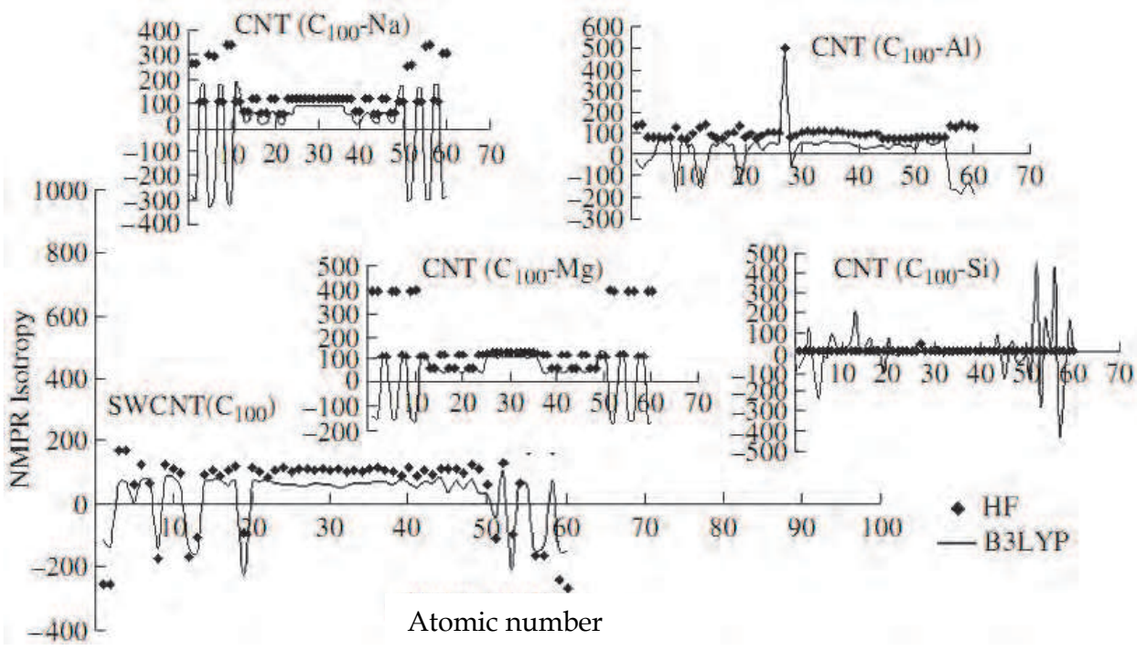

Fig. 11. NMR isotropy diagrams of SWCNT (C_{100}) for HF/6–31G (◆) and BLYP/6–31G (−) method

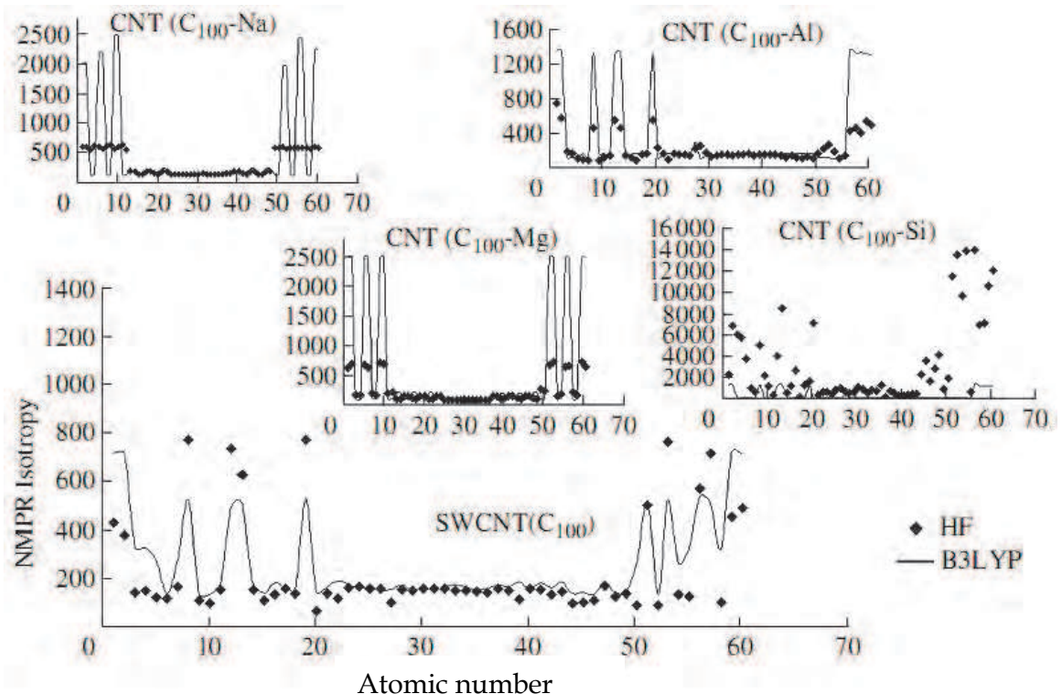

Fig. 12. NMR anisotropy diagrams of SWCNT (C100) for HF/6–31G (◆) and BLYP/6–31G (−) method

5. Conclusion

Carbon Nanotubes have been intensively studied due to their importance as building block in nanotechnology. The special geometry and unique properties of carbon Nanotube offer great potential applications, including Nanoelectronic devices, energy storage, gas sensing, chemical probe, electron transport, and biosensors, field emission display, etc. Such devices operate typically on the changes of electrical response characteristics of the Nanowire active component with the application of an externally applied mechanical stress or the adsorption of chemical or bio-molecule. For a better understanding of the physical and electronic properties of single-walled carbon Nanotubes (SWCNTs) at the Nano scale, a challenging task in theoretical calculation is needed in order to design the specific material properties because of the large size of the SWCNTs and their complicated and size dependent electronic structure. Modeling of functionalized Nanotubes and nanostructures for such technologies of SWCNTs can be greatly benefit from the first principles methods based on the density functional theory (DFT). The equilibrium position, adsorption energy, binding energy, charge transfer, and electronic band structures can be computed for different kinds of SWNTs. Effects of surrounding medium and intrinsic structural defects can also be taken into account. In this work we review some recent DFT investigation on the gas-sensing properties and the dielectric properties. Charge transfer and gas-induced charge fluctuation might significantly affect the transport properties of SWNTs. The size and chirality's of the carbon Nanotubes were typical determined from the SWCNT Raman energy spectra of a peak around 150–300 cm^{-1}, due to the radial breathing mode. Besides, the geometry and electrical properties of Nanotube are very sensitive to dielectric constants which we can observe from the normal mode analysis. A calculation method for identifying the Raman modes of SWCNTs based on the symmetry of the vibration modes has been discussed. The Raman intensity of each vibration mode varies with polarization direction, and the relationship can be expressed as analytical functions. Each Raman active mode of SWCNT can be distinguished from the group theory principle.

In section 2, with the calculation of the normal modes using the U Matrix it is possible to get the F Matrix from the multiplication of frequency to the U Matrix. Solving the determination of F Matrix versus dielectric can be useful for understanding of the electrical behavior of nanotubes in the quantitative structure activity relationship studies. The geometry and electrical properties of nanotube are very sensitive to dielectric constants. The normal modes also will be changed in the high dielectric constants.

In section 3, *Ab initio* calculations were carried out with GAUSSIAN 98 program at the HF/3-21G level of theory to investigate the effects of polar solvents and different temperatures on the stability of SWCNT in various solvents. The results obtained from Onsager model calculations are illustrated using the energy difference between these conformers which are quite sensitive to the polarity of the surrounding solvent, that the water and methanol solvents can be suggested as the most compatible solvent for studying the structural properties of SWCNT. Also orientation of the water molecules at the CNT-water interface can be affected by the orientation of the water dipole moment. Moreover, among the energy values obtained from different MM+, AMBER, and BIO+ force fields, the AMBER force field is the most proper force field for studying SWCNT.

In section 4, A Quantum Mechanics (QM) is used for investigated the nature of metals transport and interaction with single-walled carbon nanotubes (SWCNTs) inter membranes. Metal species can be transported actively by a combination of SWCNT-membranes

conducting channels that have been used for bio-molecular and detection. Ab initio calculations using DFT/B3LYP and HF levels with 6–31G and 6–31G* basis set of theory have allowed the determination of structure electronic, properties thermodynamic, magnetic properties for SWCNTs with Na, Mg, Al, and Si. NMR chemical shielding tensors in the methods framework makes it possible to study the chemical shift of specific group in carbon nanotubes in absence and presence metals. A comprehensive on effects of atoms on SWCNTs were revealed that it is on its electronic structure: 1) transfer of charge from the atom to the SWCNTs; 2) electrostatic interactions between the delocalized e electrons of the SWCNTs and atoms. The basis set used 6–31G and 6–31G* that increasing electronegativity metals increased the total energy. The proportion SWCNTs were changed by them. The results are presented for T = 310 K, the temperature of human's body. In fact, it was determined that SWCNT blocked potassium channels in a dose-dependent manner. Fullerenes were discovered to be less effective channel Blockers than CNT. The mechanism was solely dependent on the size and shape of the nano-particles. They also concluded that electrochemical interactions are between CNT and the ion channels.

6. Acknowledgment

The work has been supported by Thailand Research Fund (TRF), Thailand Center of Excellence in Physics (ThEP), Center for Innovation in Chemistry (PERCH-CIC), and the National Research University Project under Thailand's Office of the Higher Education Commission, Thailand for financial support.

7. References

Ajayan, P.M.; Stephan, O.; Colliex, C. & Trauth, D. (1994) Aligned carbon nanotube arrays formed by cutting a polymer resin-nanotube composite, *Science,* Vol.265, No.5176 (August 1994), pp. 1212-1214.

Alon, O.E. (2001) Number of raman- and infrared-active vibrations in single-walled carbon nanotubes, *Physical Review B,* Vol.63, pp. 201403-201406.

Alon, O.E. (2003) From spatial symmetry to vibrational spectroscopy of single-walled nanotubes, *Journal of Physics: Condensed Matter,* Vol.15, p. S2489, ISSN 0953-8984.

Alvarino, J.M. (1978) On the complete reduction of representations of infinite point groups, *Journal of Chemical Education,* Vol.55, p. 307.

Alvarino, J.M. & Chamorro, A. (1980) Continuous point groups: A simple derivation of the closed formula for the reduction of representations, *Journal of Chemical Education,* Vol.57, p. 785.

Bachilo, S.M.; Strano, M.S.; Kittrell, C.; Hauge, R.H.; Smalley, R.E. & Weisman, R.B. (2002) Structure-assigned optical spectra of single-walled carbon nanotubes, *Science,* Vol.298, No.5602, (December 2002), pp. 2361-2366.

Bahr, J.L.; Yang, J.; Kosynkin, D.V.; Bronikowski, M.J.; Smalley, R.E. & Tour, J.M. (2001) Functionalization of carbon nanotubes by electrochemical reduction of aryl diazonium salts: a bucky paper electrode, *Journal of the American Chemical Society,* Vol.123, pp. 6536-6542.

Banerjee, S. & Wong, S.S. (2002) Rational sidewall functionalization and purification of single-walled carbon nanotubes by solution-phase ozonolysis, *The Journal of Physical Chemistry B,* Vol.106, pp. 12144-12151.

Barone, V.; Peralta, J.E.; Wert, M.; Heyd, J. & Scuseria, G.E. (2005) Density functional theory study of optical transitions in semiconducting single-walled carbon nanotubes, *Nano Letters,* Vol.5, pp. 1621-1624.

Becke, A.D. (1993) Density-functional thermochemistry. Iii. The role of exact exchange, *The Journal of Chemical Physics,* Vol.98, pp. 5648-5652.

Becke, A.D. (1997) Density-functional thermochemistry. V. Systematic optimization of exchange-correlation functionals, *The Journal of Chemical Physics,* Vol.107, pp. 8554-8560.

Bethune, D.S.; Klang, C.H.; de Vries, M.S.; Gorman, G.; Savoy, R.; Vazquez, J. & Beyers, R. (1993) Cobalt-catalysed growth of carbon nanotubes with single-atomic-layer walls, *Nature,* Vol.363, pp. 605-607.

Cai, L.; Bahr, J.L.; Yao, Y. & Tour, J.M. (2002) Ozonation of single-walled carbon nanotubes and their assemblies on rigid self-assembled monolayers, *Chemistry of Materials,* Vol.14, pp. 4235-4241.

Collins, P.G.; Zettl, A.; Bando, H.; Thess, A. & Smalley, R.E. (1997) Nanotube nanodevice, *Science,* Vol.278, No.5335, (October 1997), pp. 100-102.

Coluci, V.R.; Galvão, D.S. & Jorio, A. (2006) Geometric and electronic structure of carbon nanotube networks: 'super'-carbon nanotubes, *Nanotechnol*, Vol.17, p. 617.

Cotton, F.A. 2nd Ed. (1971) *Chemical application of group theory*, John Wiley & Sons, ISBN 0471175706, New York, USA.

Damnjanovic, M. (1983) Standard components of polar and axial vectors for quasi one-dimensional systems, *Physics Letters A,* Vol.94, pp. 337-339.

Damnjanovic, M.; Miloscaronevic, I.; Vukovic, T. & Sredanovic, R. (1999) Full symmetry, optical activity, and potentials of single-wall and multiwall nanotubes, *Physical Review B,* Vol.60, pp. 2728-2739.

Damnjanovic, M.; Vukovic, T. & Milosevic, I. (2000) Modified group projectors: Tight-binding method, *Journal of Physics A: Mathematical and General,* Vol.33, p. 6561.

Dresselhaus, M.S.; Dresselhaus, G. & Jorio, A. (2006) *Applications of Group Theory to the Physics of Condensed Matter*, Springer, ISBN 978-3-540-32897-1, Heidelberg, Germany.

de Heer, W.A.; Châtelain, A. & Ugarte, D. (1995) A carbon nanotube field-emission electron source, *Science,* Vol.270, No.5239, (November 1995), pp. 1179-1180.

Eklund, P.C.; Holden, J.M. & Jishi, R.A. (1995) Vibrational modes of carbon nanotubes; spectroscopy and theory, *Carbon,* Vol.33, pp. 959-972.

Flurry, R.L. (1979) On the characters and representations of continuous point groups, *Journal of Chemical Education,* Vol.56, p. 638.

Ganjali M.R.; Norouzi, P.; Rezapour, M.; Faridbod, F. & Pourjavid, M. R. (2006). Supramolecular based membrane sensors. *Sensors*, Vol.8, pp. 1018-1086.

Hartschuh, A.; Pedrosa, H.N.; Peterson, J.; Huang, L.; Anger, P.; Qian, H.; Meixner, A.J.; Steiner, M.; Novotny, L. & Krauss, T.D. (2005) Single carbon nanotube optical spectroscopy, *ChemPhysChem,* Vol.6, pp. 577-582.

Herrera, J.E. & Resasco, D.E. (2003) In situ tpo/raman to characterize single-walled carbon nanotubes, *Chemical Physics Letters,* Vol.376, pp. 302-309.

Holzinger, M.; Abraham, J.; Whelan, P.; Graupner, R.; Ley, L.; Hennrich, F.; Kappes, M. & Hirsch, A. (2003) Functionalization of single-walled carbon nanotubes with (r-)oxycarbonyl nitrenes, *Journal of the American Chemical Society,* Vol.125, pp. 8566-8580.

Huang, J.Y.; Chen, S.; Ren, Z.F.; Chen, G. & Dresselhaus, M.S. (2006) Real-time observation of tubule formation from amorphous carbon nanowires under high-bias joule heating, *Nano Letters,* Vol.6, pp. 1699-1705.

HyperChem 7.0 (2001), Hypecube Inc., Florida, USA.

Jorio, A.; Saito, R.; Hafner, J.H.; Lieber, C.M.; Hunter, M.; McClure, T.; Dresselhaus, G. & Dresselhaus, M.S. (2001) Structural (n, m) determination of isolated single-wall carbon nanotubes by resonant raman scattering, *Physical Review Letters,* Vol.86, pp. 1118-1121.

Jorio, A.; Fantini, C.; Pimenta, M.A.; Capaz, R.B.; Samsonidze, G.G.; Dresselhaus, G.; Dresselhaus, M.S.; Jiang, J.; Kobayashi, N.; Gr; uuml; neis, A. & Saito, R. (2005) Resonance raman spectroscopy (n,m) –dependent effects in small-diameter single-wall carbon nanotubes, *Physical Review B,* Vol.71, pp. 075401-075412.

Kane, C.L. & Mele, E.J. (1997) Size, shape, and low energy electronic structure of carbon nanotubes, *Physical Review Letters,* Vol.78, pp. 1932-35.

Kar, T.; Akdim, B.; Duan, X. & Pachter, R. (2006) Open-ended modified single-wall carbon nanotubes: A theoretical study of the effects of purification, *Chemical Physics Letters,* Vol.423, pp. 126-130.

Kazaoui, S.; Minami, N.; Jacquemin, R.; Kataura, H. & Achiba, Y. (1999) Amphoteric doping of single-wall carbon-nanotube thin films as probed by optical absorption spectroscopy, *Physical Review B,* Vol.60, pp. 13339-13342.

Kürti, J.; Zólyomi, V.; Kertesz, M.; Sun, G.; Baughman, R.H. & Kuzmany, H. (2004) Individualities and average behavior in the physical properties of small diameter single-walled carbon nanotubes, *Carbon,* Vol.42, pp. 971-978.

Lee, C.; Yang, W. & Parr, R.G. (1988) Development of the colle-salvetti correlation-energy formula into a functional of the electron density, *Physical Review B,* Vol.37, pp. 785-789.

Lee, V.; Nimmanpipug, P.; Mollaamin, F.; Kungwan, N.; Thanasanvorakun, S. & Monajjemi, M. (2009) Investigation of single wall carbon nanotubes electrical properties and normal mode analysis: Dielectric effects, *Russian Journal of Physical Chemistry A, Focus on Chemistry,* Vol.83, pp. 2288-2296.

Liu, J.C. & Monson, P.A. (2005) Molecular modeling of adsorption in activated carbon: Comparison of monte carlo simulations with experiment, *Adsorption,* Vol.11, pp. 5-13.

Martinez; M, T.; Callejas; M, A.; Benito; A, M.; Cochet; M; Seeger; T; Anson; A; Schreiber; J; Gordon; C; Marhic; C; Chauvet; O; Maser & W. K. (2003) Modifications of single-wall carbon nanotubes upon oxidative purification treatments, *Nanotechnology,* Vol.14, 691-695.

Maultzsch, J.; Telg, H.; Reich, S. & Thomsen, C. (2005) Radial breathing mode of single-walled carbon nanotubes: Optical transition energies and chiral-index assignment, *Physical Review B,* Vol.72, pp. 205438-205454.

Mickelson, E.T.; Huffman, C.B.; Rinzler, A.G.; Smalley, R.E.; Hauge, R.H. & Margrave, J.L. (1998) Fluorination of single-wall carbon nanotubes, *Chemical Physics Letters,* Vol.296, pp. 188-194.

Monajjemi, M.; Baei, M. & Mollaamin, F. (2008a) Quantum mechanics study of hydrogen chemisorptions on nanocluster vanadium surface, *Russian Journal of Inorganic Chemistry,* Vol.53, pp. 1430-1437.

Monajjemi, M.; Mahdavian, L. & Mollaamin, F. (2008b) Characterization of nanocrystalline silicon germanium film and nanotube in adsorption gas by Monte Carlo and Langevin dynamic simulation, *Bulletin of the Chemical Society of Ethiopia,* Vol.22, No.2, pp. 277-286, ISSN: 1011-3924.

Monajjemi, M.; Mahdavian, L.; Mollaamin, F. & Khaleghian, M. (2009) Interaction of na, mg, al, si with carbon nanotube (cnt): Nmr and ir study, *Russian Journal of Inorganic Chemistry,* Vol.54, pp. 1465-1473.

Monajjemi, M.; Khaleghian, M.; Tadayonpour, N. & Mollaamin, F. (2010) The Effect of Different Solvents and Temperatures on Stability of Single-Walled Carbon Nanotube: a QM/MD Study, *International Journal of Nanoscience*, Vol.9, pp. 517-529.

Mora-Diez, N.; Senent, M.L. & Garcia, B. (2006) Ab initio study of solvent effects on the acetohydroxamic acid deprotonation processes, *Chemical Physics,* Vol.324, pp. 350-358.

Nardelli, M. B.; Yakobson, B.I. & Bernholc, J. (1998) Mechanism of strain release in carbon nanotubes, *Physical Review B,* Vol.57, pp. R4277-4280.

Odom, T.W.; Huang, J.-L.; Kim, P. & Lieber, C.M. (1998) Atomic structure and electronic properties of single-walled carbon nanotubes, *Nature,* Vol.391, pp. 62-64.

Ouyang, M.; Huang, J.-L. & Lieber, C.M. (2002) Fundamental electronic properties and applications of single-walled carbon nanotubes, *Accounts of Chemical Research,* Vol.35, pp. 1018-1025.

Pelletier, M.J. (1999) *Analytical Applications of Raman Spectroscopy*, Kaiser Optical Systems Inc., ISBN 0632053054, Michigan, USA.

Peng, H.; Alemany, L.B.; Margrave, J.L. & Khabashesku, V.N. (2003) Sidewall carboxylic acid functionalization of single-walled carbon nanotubes, *Journal of the American Chemical Society,* Vol.125, pp. 15174-15182.

Pfeiffer, R.; Kuzmany, H.; Kramberger, C.; Schaman, C.; Pichler, T.; Kataura, H.; Achiba, Y.; Kürti, J., and Zólyomi, V. (2003) Unusual high degree of unperturbed environment in the interior of single-wall carbon nanotubes, *Physical Review Letters,* Vol.90, p. 225501.

Saito, R.; Dresselhaus, G. & Dresselhaus, M.S. (1992a) Topological defects in large fullerenes, *Chemical Physics Letters,* Vol.195, pp. 537-542.

Saito, R.; Fujita, M.; Dresselhaus, G. & Dresselhaus, M.S. (1992b) Electronic structure of graphene tubules based on C_{60}, *Physical Review B,* Vol.46, pp. 1804-1811.

Saito, Y.; Hamaguchi, K.; Hata, K.; Uchida, K.; Tasaka, Y.; Ikazaki, F.; Yumura, M.; Kasuya, A. & Nishina, Y. (1997) Conical beams from open nanotubes, *Nature,* Vol.389, pp. 554-555.

Saito, R.; Takeya, T.; Kimura, T.; Dresselhaus, G. & Dresselhaus, M.S. (1998) Raman intensity of single-wall carbon nanotubes, *Physical Review B,* Vol.57, pp. 4145-4153.

Spire, T. & Brown R. M. (February 1996). High Resolution TEM Observations of Single Walled Carbon Nanotubes,Availble from http://www.botany.utexas.edu/facstaff/facpages/mbrown/ongres/tspires/nano.htm.

Strano, M.S.; Dyke, C.A.; Usrey, M.L.; Barone, P.W.; Allen, M.J.; Shan, H.; Kittrell, C.; Hauge, R.H.; Tour, J.M. & Smalley, R.E. (2003) Electronic structure control of single-walled carbon nanotube functionalization, *Science,* Vol.301, No.5639, (September 12, 2003), pp. 1519-1522.

Schafer, L. & Cyvin, S.J. (1971) Complete reduction of representations of infinite point groups, *Journal of Chemical Education,* Vol.48, p. 295.

Strommen, D.P. & Lippincott, E.R. (1972) Comments of infinite point groups, *Journal of Chemical Education,* Vol. 49, p. 341.

Strommen, D.P. (1979) Some additional comments on infinite point groups, *Journal of Chemical Education,* Vol.56, p. 640.

Tagmatarchis, N. & Prato, M. J. (2004) Mater. Chem. Vol.14, No.4, p. 437.

Tiana, G.; Sutto, L. & Broglia, R.A. (2007) Use of the metropolis algorithm to simulate the dynamics of protein chains, *Physica A: Statistical Mechanics and its Applications,* Vol.380, pp. 241-249.

Umek, P.; Seo, J.W.; Hernadi, K.; Mrzel, A.; Pechy, P.; Mihailovic, D.D. & Forró, L. (2003) Addition of carbon radicals generated from organic peroxides to single wall carbon nanotubes, *Chemistry of Materials,* Vol.15, pp. 4751-4755.

Wang, W. & Skeel, R. D. (2003) Analysis of a few numerical integration methods for the Langevin equation, *Molecular Phys*ics Vol.101, No.14, pp. 2149-2156.

Wilder, J.W.G.; Venema, L.C.; Rinzler, A.G.; Smalley, R.E. & Dekker, C. (1998) Electronic structure of atomically resolved carbon nanotubes, *Nature,* Vol.391, pp. 59-62.

Wilson, E.B.; Decius, J.C. & Cross, P.C. (1955). *Molecular vibrations : The theory of infrared and raman vibrational spectra*, McGraw-Hill, New York, USA

Witanowski, M.; Biedrzycka, Z.; Sicinska, W. & Grabowski, Z. (2002) A study of solvent polarity and hydrogen bonding effects on the nitrogen nmr shieldings of n-nitramines and ab initio calculations of the nitrogen shieldings of c-nitro, n-nitro and o-nitro systems, *Journal of Molecular Structure,* Vol.602-603, pp. 199-207.

Yumura, T.; Nozaki, D.; Bandow, S.; Yoshizawa, K. & Iijima, S. (2005) End-cap effects on vibrational structures of finite-length carbon nanotubes, *Journal of the American Chemical Society,* Vol.127, Aug 24, pp. 11769- 11776, ISSN 0002-7863.

Zhang, M.; Fang, S.; Zakhidov, A.A.; Lee, S.B.; Aliev, A.E.; Williams, C.D.; Atkinson, K.R. & Baughman, R.H. (2005) Strong, transparent, multifunctional, carbon nanotube sheets, *Science,* Vol.309, August 19, pp. 1215-1219, ISSN 1095-9203.

Zhou, Z.; Steigerwald, M.; Hybertsen, M.; Brus, L. & Friesner, R.A. (2004) Electronic structure of tubular aromatic molecules derived from the metallic (5,5) armchair single wall carbon nanotube, *Journal of the American Chemical Society,* Vol.126, pp. 3597-3607.

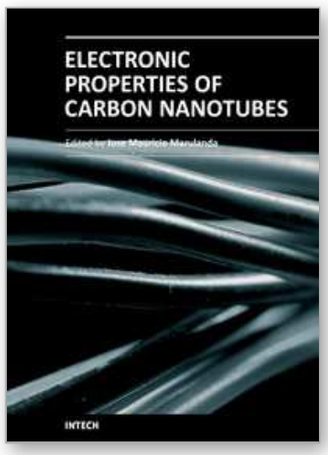

Electronic Properties of Carbon Nanotubes

Edited by Prof. Jose Mauricio Marulanda

ISBN 978-953-307-499-3
Hard cover, 680 pages
Publisher InTech
Published online 27, July, 2011
Published in print edition July, 2011

Carbon nanotubes (CNTs), discovered in 1991, have been a subject of intensive research for a wide range of applications. These one-dimensional (1D) graphene sheets rolled into a tubular form have been the target of many researchers around the world. This book concentrates on the semiconductor physics of carbon nanotubes, it brings unique insight into the phenomena encountered in the electronic structure when operating with carbon nanotubes. This book also presents to reader useful information on the fabrication and applications of these outstanding materials. The main objective of this book is to give in-depth understanding of the physics and electronic structure of carbon nanotubes. Readers of this book should have a strong background on physical electronics and semiconductor device physics. This book first discusses fabrication techniques followed by an analysis on the physical properties of carbon nanotubes, including density of states and electronic structures. Ultimately, the book pursues a significant amount of work in the industry applications of carbon nanotubes.

InTech Europe
University Campus STeP Ri
Slavka Krautzeka 83/A
51000 Rijeka, Croatia
Phone: +385 (51) 770 447
Fax: +385 (51) 686 166
www.intechopen.com

InTech China
Unit 405, Office Block, Hotel Equatorial Shanghai
No.65, Yan An Road (West), Shanghai, 200040, China
中国上海市延安西路65号上海国际贵都大饭店办公楼405单元
Phone: +86-21-62489820
Fax: +86-21-62489821

IntechOpen